ARTICLE

doi:10.1038/nature17938

Continuous evolution of *Bacillus thuringiensis* toxins overcomes insect resistance

Ahmed H. Badran[1,2], Victor M. Guzov[3], Qing Huai[3], Melissa M. Kemp[3], Prashanth Vishwanath[3], Wendy Kain[4], Autumn M. Nance[5], Artem Evdokimov[5]†, Farhad Moshiri[5], Keith H. Turner[5], Ping Wang[4], Thomas Malvar[5] & David R. Liu[1,2]

The *Bacillus thuringiensis* δ-endotoxins (Bt toxins) are widely used insecticidal proteins in engineered crops that provide agricultural, economic, and environmental benefits. The development of insect resistance to Bt toxins endangers their long-term effectiveness. Here we have developed a phage-assisted continuous evolution selection that rapidly evolves high-affinity protein–protein interactions, and applied this system to evolve variants of the Bt toxin Cry1Ac that bind a cadherin-like receptor from the insect pest *Trichoplusia ni* (TnCAD) that is not natively bound by wild-type Cry1Ac. The resulting evolved Cry1Ac variants bind TnCAD with high affinity (dissociation constant $K_d = 11–41$ nM), kill TnCAD-expressing insect cells that are not susceptible to wild-type Cry1Ac, and kill Cry1Ac-resistant *T. ni* insects up to 335-fold more potently than wild-type Cry1Ac. Our findings establish that the evolution of Bt toxins with novel insect cell receptor affinity can overcome insect Bt toxin resistance and confer lethality approaching that of the wild-type Bt toxin against non-resistant insects.

The expression of insecticidal proteins from *B. thuringiensis* (Bt toxins) in crops has proved to be a valuable strategy for agricultural pest management[1]. Bt-toxin-producing crops have been widely adopted in agriculture with substantial economic and environmental benefits[2], and have increased global agricultural productivity by an estimated US$78 billion from 1996 to 2013 (ref. 3). Unfortunately, Bt toxin resistance has evolved among insect pests and threatens the continued success of this strategy for pest control[4]. While resistance management strategies have been developed, including the use of multiple Bt toxins and preserving susceptible alleles in insect populations, the evolution of insect resistance to Bt toxins remains the most serious current threat to sustaining the gains offered by transgenic crops[4].

Bt toxins interact with protein receptors on the surface of insect midgut cells, leading to pore formation in the cell membrane and cell death[5]. Bt toxin resistance is commonly associated with the mutation, downregulation, or deletion of these receptors[2]. We hypothesized that it might be possible to overcome Bt toxin resistance by evolving novel Bt toxins that bind with high affinity to new gut cell receptor proteins in insects. If successful, such an approach has the potential to alter toxin specificity, improve toxin potency, and bypass receptor-related resistance mechanisms.

Here we use phage-assisted continuous evolution (PACE) to rapidly evolve Bt toxins through more than 500 generations of mutation, selection, and replication to bind a new receptor expressed on the surface of insect midgut cells. PACE-derived Bt toxins bind the new receptor with high affinity and specificity, induce target receptor-dependent lysis of insect cells, and enhance the insecticidal activity against both sensitive and Bt-resistant insect larvae up to 335-fold. Collectively, these results establish an approach to overcoming Bt toxin resistance and provide a new platform for the rapid evolution of other protein-binding biomolecules.

Development of protein–binding PACE

PACE has mediated the rapid laboratory evolution of diverse protein classes including polymerases, proteases, and genome-editing proteins, yielding variants with highly altered activities and specificities[6–12]. While PACE has not been previously used to evolve protein-binding activity, we speculated that the bacterial two-hybrid system[13] could serve as the basis of a protein-binding PACE selection (Fig. 1a). Target binding results in localization of RNA polymerase upstream of a reporter gene, initiating gene expression. To adapt this system into a protein-binding selection for PACE, we envisioned that protein:target binding could instead activate the expression of the filamentous bacteriophage gene III, which is required for the infectivity of progeny phage[6] (Fig. 1b).

To maximize the sensitivity of the bacterial two-hybrid, we extensively optimized parameters including (1) transcriptional activation and DNA-binding domains, (2) protein expression level, (3) interaction binding affinity, (4) DNA-binding domain multivalency state, (5) reporter gene ribosome-binding site, (6) operator–promoter distance, (7) RNA polymerase–promoter affinity, and (8) DNA-binding domain–bait linker length. While the previously described bacterial two-hybrid system yielded a 17-fold increase in transcriptional activation using a model high-affinity interaction (HA4 monobody binding to the SH2 domain of ABL1 kinase)[14], our optimized system enhanced transcriptional activation >200-fold using the same interaction (Extended Data Figs 1–3). This system consists of the *Escherichia coli* RNA polymerase omega subunit (RpoZ) as the activation domain, the 434 phage cI repressor as the DNA-binding domain, and an optimized P_{lacZ}-derived promoter ($P_{lacZ\text{-}opt}$) to drive reporter transcription. Together, these results extend and improve previously described bacterial systems[13] that transduce protein-target binding into gene expression in a manner that can be tuned by the researcher.

[1]Department of Chemistry and Chemical Biology, Harvard University, Cambridge, Massachusetts 02138, USA. [2]Howard Hughes Medical Institute, Harvard University, Cambridge, Massachusetts 02138, USA. [3]Monsanto Company, 245 First Street, Suite 200, Cambridge, Massachusetts 02142, USA. [4]Department of Entomology, Cornell University, Geneva, New York 14456, USA. [5]Monsanto Company, 700 Chesterfield Parkway West, Chesterfield, Missouri 63017, USA. †Present address: HarkerBIO, 700 Ellicott Street, Buffalo, New York 14023, USA.

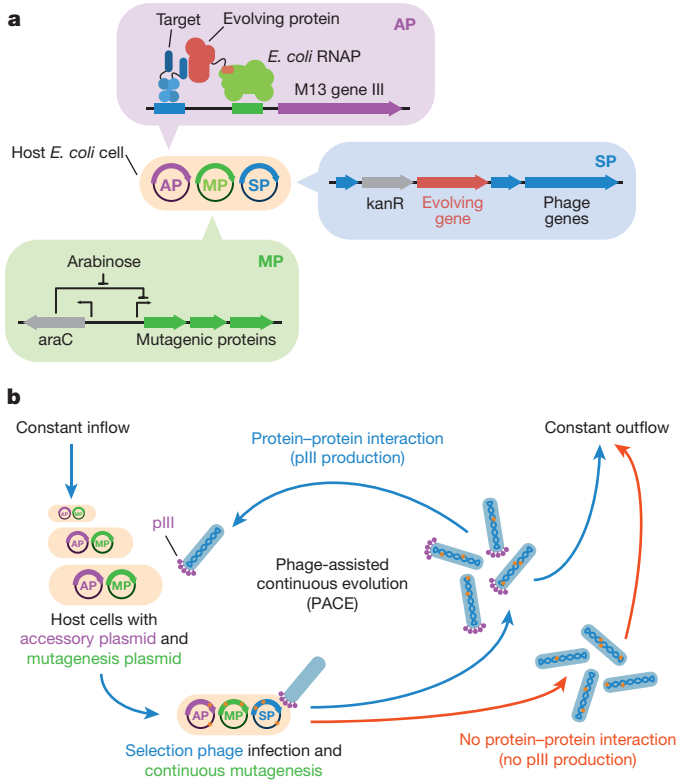

Figure 1 | Protein-binding PACE. a, Anatomy of a phage-infected host cell during PACE. The host *E. coli* cell carries two plasmids: the accessory plasmid (AP)[6], which links protein binding to phage propagation and controls selection stringency, and the mutagenesis plasmid (MP)[6,12], which enables arabinose-inducible elevated levels of mutagenesis during PACE. **b**, After infection, each selection phage (SP) that encodes an evolving protein capable of binding to the target protein induces expression of gene III from the accessory plasmid, resulting in the production of pIII, a phage protein required for progeny phage produced by that host cell to infect subsequent host cells. PACE takes place in a fixed-volume vessel (the 'lagoon') that is continuously diluted with fresh host cells. Only those selection phages encoding proteins that bind the target can propagate faster than they are diluted out of the lagoon.

The HA4 monobody binds to the SH2 domain of ABL1 kinase ($K_d = 7$ nM)[14]. The mutant HA4 Y87A monobody binds the ABL1 SH2 domain with 100- to 1,000-fold weaker affinity[14]. Whereas wild-type HA4 monobody fused to RpoZ in the presence of 434cI–SH2 resulted in potent transcriptional activation in our optimized bacterial two-hybrid system, transcriptional activation using $HA4_{Y87A}$ was negligible (Fig. 2a). Similarly, selection phage expressing the *rpoZ–HA4* fusion robustly propagate using host cell strains carrying accessory plasmids expressing the *434cI–SH2* fusion, whereas a selection phage encoding *rpoZ–*$HA4_{Y87A}$ did not support phage propagation. These findings demonstrate that the Y87A mutant HA4 monobody does not support gene III expression or phage propagation (Extended Data Fig. 3).

To validate protein-binding PACE, we challenged the system to evolve a functional SH2-binding monobody starting from the $HA4_{Y87A}$ mutant. To revert the $HA4_{Y87A}$ mutant back to a Tyr87 protein requires three adjacent point mutations (GCG to TAT or TAC). The *rpoZ–*$HA4_{Y87A}$ selection phage was propagated during PACE for 66 h in the absence of selection pressure (that is, allowing evolutionary drift[9]), before engaging selection pressure by changing the host cell strain to one requiring SH2 binding-dependent phage propagation (Fig. 2b). Under selection pressure, control lagoons that previously experienced neither drift nor mutagenesis, or that experienced only mutagenesis, quickly lost their selection phages encoding the evolving monobody population (phage 'wash out'). In contrast, lagoons subjected to both drift and mutagenesis dropped markedly in phage titre for the first 12 h, but recovered over the next 24 h (Fig. 2c). Sequence analysis of eight phage clones surviving 48 h of PACE revealed that all eight evolved either Tyr or Trp at HA4 position 87 (Fig. 2c), either of which restored transcriptional activation (Extended Data Fig. 3). These results demonstrate that protein-binding PACE can rapidly evolve proteins with target affinity, even when multiple mutations are required to gain protein-binding activity.

Bt toxin target receptor design

Binding of Bt toxins to protein receptors on insect midgut cells is a critical event in the mechanism of insecticidal activity[5,15]. To develop a strategy to overcome Bt toxin resistance, we sought to evolve Cry1Ac, a widely used Bt toxin, to bind TnCAD, an insect cell membrane cadherin-like receptor from cabbage looper (*T. ni*) that is not natively bound by wild-type Cry1Ac (see Supplementary Discussion). *T. ni* has developed Bt resistance in agricultural settings and has been widely studied for insect resistance to Bt toxins[2].

Previous studies of Cry1Ac binding to cadherin-like receptor proteins from Lepidoptera identified multiple putative toxin binding regions (TBRs) in the cadherin[16,17]. The homologous region of the TBR in TnCAD differs from that of cadherin-like proteins from other lepidopteran species at seven amino-acid positions (Extended Data Fig. 4). To create an evolutionary stepping-stone from cadherin-like proteins that bind Cry1Ac to TnCAD, three residues (F1433, S1436, and A1437) from the TBR of four other lepidopteran species[18–21] were introduced into TnCAD, resulting in an artificial receptor fragment designated TnTBR3 (Extended Data Fig. 4). We constructed accessory plasmids expressing various TnTBR3 fragments fused to 434cI and assessed transcriptional activation levels in the presence of various domains of Cry1Ac fused to RpoZ (Extended Data Fig. 4). Only Cry1Ac containing three domains of the active toxin (residues 1–609) showed weak binding activity for TnTBR3 fragment 3 (TnTBR3-F3) (Extended Data Fig. 4). A selection phage carrying the *rpoZ–Cry1Ac* fusion gene replicated ~100-fold in a host strain carrying the TnTBR3-F3 accessory plasmid after propagation overnight, whereas a control selection phage lacking the *rpoZ–Cry1Ac* fusion did not replicate (Extended Data Fig. 4). These observations identified TnTBR3-F3 as a promising evolutionary stepping-stone to serve as a starting target for continuous evolution in PACE.

Evolution of Cry1Ac to bind TnCAD

We performed 528 h of PACE on Cry1Ac in four segments while varying mutagenesis levels and selection stringency (Fig. 3a). For the first two segments (0–144 h and 144–276 h), the accessory plasmid expressed the TnTBR3-F3 stepping-stone target fused to 434cI. For the final two segments of PACE (276–396 h and 396–528 h), the accessory plasmid expressed the TnCAD-F3 final target fused to 434cI. To enhance mutagenesis, we used the moderate-potency mutagenesis plasmid MP4 (ref. 12) during PACE for binding to TnTBR3-F3 (PACE segments 1 and 2) in an effort to decrease the likelihood of accessing early mutations that could impair essential features of Cry1Ac beyond target receptor binding. During the final two PACE segments for binding to TnCAD-F3 (PACE segments 3 and 4) we used MP6, which induces a greater mutation rate and broader mutational spectrum than MP4 (ref. 12), as phage washout consistently occurred during TnCAD-F3 PACE attempts with MP4, suggesting that higher levels of mutagenesis were required to access rare Cry1Ac mutational combinations that conferred binding to the final TnCAD-F3 target. We increased selection stringency during PACE by increasing lagoon flow rates and reducing the number of TnTBR3-F3 or TnCAD-F3 fragments participating in Cry1Ac variant recognition (Fig. 2a and Extended Data Fig. 3). Phage surviving 528 h of PACE experienced on average 511 generations of mutagenic replication under selection conditions[6].

Sequencing of individual clones at the end of the first PACE segment (144 h; four copies of TnTBR3-F3 per $P_{lacZ\text{-}opt}$ promoter) revealed a strong consensus of two coding mutations in *Cry1Ac*, and one coding

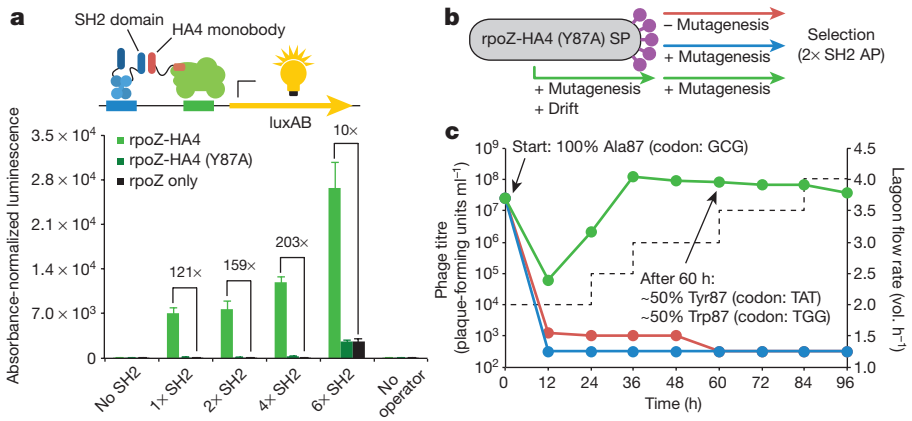

Figure 2 | Protein-binding PACE selection development and stringency modulation. a, The relationship between target protein multivalency and transcriptional output measured by luciferase expression. The number of ABL1 SH2 domains available to bind the HA4 monobody was modulated by varying the 434cI DNA-binding domain multivalency state (1×, 2×, 4×, or 6× SH2). 'No operator' indicates a scrambled 434cI operator control accessory plasmid. **b**, During PACE, the inactive monobody mutant $HA4_{Y87A}$ was subjected to no mutagenesis (mutagenesis plasmid not induced), enhanced mutagenesis (mutagenesis plasmid induced with arabinose), or enhanced mutagenesis with genetic drift (mutagenesis plasmid induced with arabinose in addition to an initial period of zero selection stringency), then selected for binding to the ABL1 SH2 target protein. **c**, The combination of drift and enhanced mutagenesis during PACE (green line) resulted in the evolution of Tyr and Trp residues at position 87, either of which restores SH2-binding activity, while no mutagenesis (red line) or enhanced mutagenesis without drift (blue line) resulted in phage washout. Error bars in **a**, s.d. of at least three independent biological replicates.

mutation in *rpoZ* (Extended Data Fig. 5). The three mutations together resulted in 11-fold higher transcriptional activation than that of the wild-type *rpoZ–Cry1Ac* fusion. At the end of the second segment (276 h; two copies of TnTBR3-F3 per $P_{lacZ\text{-}opt}$ promoter), even greater degrees of transcriptional activation were observed, up to 20-fold higher than the level resulting from the starting fusion protein (Fig. 3b and Extended Data Fig. 5). At the end of third segment (396 h; four copies of TnCAD-F3 per $P_{lacZ\text{-}opt}$ promoter), Cry1Ac variants evolved with greatly enhanced apparent affinity for TnCAD-F3 (Fig. 3c and Extended Data Fig. 5). Whereas wild-type Cry1Ac could not detectably activate transcription when challenged to bind TnCAD-F3, single Cry1Ac variants emerging from a total of 384 h of PACE robustly activated transcription up to 210-fold above background in the absence of Cry1Ac variant expression. The end of the fourth segment (528 h; one copy of TnCAD-F3 per $P_{lacZ\text{-}opt}$ promoter) yielded Cry1Ac mutants that could activate transcription when challenged to bind TnCAD-F3 by up to 500-fold (Fig. 3c and Extended Data Fig. 5), consistent with strong binding to the TnCAD-F3 final target.

Characterization of evolved Cry1Ac variants

DNA sequencing of individual clones surviving 528 h of PACE revealed several consensus genotypes carrying up to 16 mutations per clone out of 22 consensus mutations, most of which localize to domain II, the predicted cadherin-binding domain of Cry1Ac (Extended Data Figs 4 and 5). To illuminate the evolution trajectories en route to TnCAD-F3 binding activity, we analysed all lagoon samples, by high-throughput DNA sequencing using both shorter-read (Illumina) and longer-read (Pacific Biosciences) methods (Extended Data Fig. 6). These efforts identified 25 mutations commonly occurring over the 528 h of PACE (Extended Data Figs 5 and 6). Oligotyping analysis[22] of the long-read data revealed plausible evolutionary trajectories over the entire course of the experiment (Fig. 3d, e). While PACE does not explicitly promote recombination as a mechanism of gene diversification, we observed multiple putative recombination events during the course of Cry1Ac evolution (Fig. 3e). These recombination events, which we presume arose from multiple phage occasionally infecting the same host cell, yielded seminal, highly functional new variants.

On the basis of our mutational analysis, we designed and synthesized consensus Cry1Ac variants containing the most commonly observed mutations (Fig. 4a, b). Purified activated Cry1Ac variants encoding PACE-derived consensus mutations bind strongly (K_d = 18–34 nM) to a TnCAD fragment containing the TBR (TnCAD-FL; Extended Data Fig. 4) by ForteBio bio-layer interferometry analysis, with evolved Cry1Ac variants C03 and C05 exhibiting the highest binding affinities (Fig. 4a and Supplementary Table 1). In contrast, wild-type Cry1Ac exhibited no significant affinity for TnCAD-FL (K_d > 1 mM) under the same conditions. These results together establish the ability of protein-binding PACE to rapidly evolve extensively mutated proteins with high target affinity.

Cry1Ac is proteolytically activated in the insect midgut[2]. The evolved consensus mutants, however, exhibited extensive proteolysis by trypsin under conditions in which the wild-type Cry1Ac was cleanly cleaved into its active form (Fig. 4c). Thermal melting studies confirmed this reduced stability (consensus variants: melting temperature T_m = ~45 °C; wild-type Cry1Ac: T_m = 71 °C; Supplementary Table 1). Despite this lower stability, trypsin-activated consensus variants robustly killed Sf9 cells expressing TnCAD, whereas wild-type Cry1Ac did not exhibit toxicity (Fig. 4d). Moreover, these evolved consensus Cry1Ac mutants showed insecticidal activity in *T. ni* larvae, although they were less potent than wild-type Cry1Ac (Fig. 4e).

We hypothesized that a subset of the consensus mutations were impairing apparent toxin potency against insect larvae by decreasing Cry1Ac stability and thus promoting degradation in insect gut. We generated Cry1Ac variants containing combinatorial reversions of the identified consensus mutations (Fig. 4b and Supplementary Table 1) and identified mutations D384Y and S404C, two mutations that arose early during PACE against the TnTBR3 stepping-stone target (Figs 3d, e and 5a), as the source of reduced protein stability. Variants lacking these two mutations, but containing the other seven consensus C05 mutations, exhibited greatly improved stability (T_m = ~60 °C). Variants lacking D384Y and S404C also exhibited proteolytic resistance similar to that of wild-type Cry1Ac, while retaining high binding affinity to TnCAD-FL (K_d = 11–41 nM) (Fig. 5a, b and Supplementary Table 1).

We assayed the toxicity of two evolved consensus Cry1Ac variants (C05 and C03) and three stabilized evolved consensus Cry1Ac variants (C05s, C03s, and A01s) lacking D384Y and S404C to cultured Sf9 insect cells expressing an ABCC2 receptor (positive control) or TnCAD. The stabilized evolved Cry1Ac variants retain their ability to bind to the ABCC2 receptor, while acquiring the ability to potently kill Sf9 cells expressing TnCAD, in contrast to the ability of wild-type Cry1Ac to only kill cells expressing the ABCC2 receptor, but not cells expressing TnCAD (Fig. 5c).

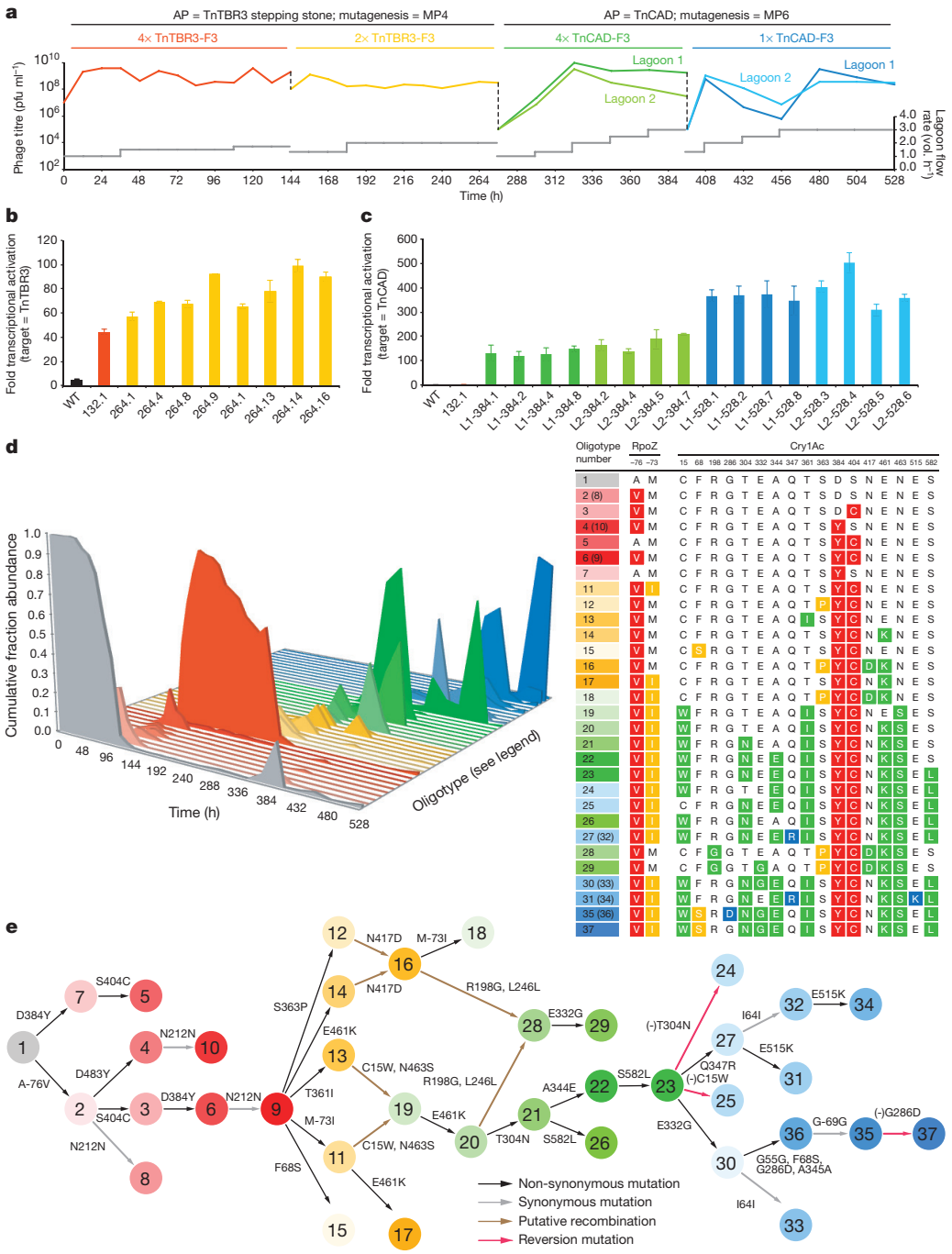

Figure 3 | Continuous evolution of Cry1Ac variants that bind the *T. ni* cadherin receptor. **a**, PACE was executed in four segments. The first two segments implemented the designed TnTBR3-F3 'stepping-stone' target under intermediate levels of mutagenesis (MP4). The final two segments implemented the final TnCAD-F3 target under high levels of mutagenesis (MP6). Phage titre (coloured lines) and lagoon flow rate (grey lines) are shown at all sampled time points. The dotted lines indicate transfer of evolving phage to a new lagoon fed by the host cell culture corresponding to the next segment of PACE. **b**, **c**, Transcriptional activation assays using 434cI–TnTBR3-F3 (**b**) or 434cI–TnCAD-F3 (**c**) and individual RpoZ–Cry1Ac variants evolved during PACE, compared with wild-type RpoZ–Cry1Ac (WT). **d**, Oligotyping analysis of lagoon samples during PACE on the basis of high-throughput DNA sequencing data. Oligotypes containing high frequency mutations (≥1%) are represented by different polygons, coloured on the basis of the stage in which they first became abundant in the evolving Cry1Ac gene pool. Mutations in Cry1Ac for each oligotype are shown in the table. Numbers in parentheses indicate the oligotype number assigned to that mutant after a synonymous (silent) mutation. **e**, Plausible evolution trajectories over the entire PACE experiment derived from oligotyping analysis strongly suggests instances of recombination during PACE, and reveals the influence of mutation rate, selection stringency, and target protein on evolutionary outcomes. The colours and numbers in each circle correspond to those in **d**.

In vivo activity of evolved Cry1Ac variants

Finally, we assayed the insecticidal activity of the stabilized evolved Cry1Ac variants against Cry1Ac-sensitive *T. ni* larvae when added to their diet. Consistent with the *in vitro* results, the stabilized evolved Cry1Ac variants exhibited substantially increased toxicity to *T. ni* larvae compared with that of the consensus-evolved Cry1Ac mutants before stabilization (Fig. 5d). Interestingly, the stabilized evolved Cry1Ac variants also exhibited insecticidal potency against susceptible *T. ni* up to fourfold higher than that of wild-type Cry1Ac, suggesting that the evolved affinity of the toxins to a new receptor may augment their insecticidal potency, even against insects susceptible to wild-type Cry1Ac. These results also suggest that the evolution of Bt toxins that recognize novel receptors could expand the range of insects that can be targeted by Bt toxins, consistent with previous *in vitro* studies[23,24] using designed Bt toxin derivatives.

Next we evaluated the insecticidal activity of the stabilized evolved Cry1Ac variants against Cry1Ac-resistant *T. ni* larvae. *T. ni* resistance to Cry1Ac has been genetically mapped to the *ABCC2* transporter gene and downregulation of expression of *APN1* (refs 25, 26), and is known to be independent of alteration of the cadherin-like receptor[27]. In this study, we also confirmed that wild-type Cry1Ac does not bind the TBR in TnCAD (see above), consistent with the previous finding that Cry1Ac does not bind TnCAD in *T. ni* midgut cell membranes[25,27,28]. Indeed, we observed ~1,000-fold lower potency of wild-type Cry1Ac against a Cry1Ac-resistant *T. ni* strain than the potency of wild-type Cry1Ac against susceptible *T. ni*[29] (Fig. 5e). Compared with wild-type Cry1Ac, stabilized evolved Cry1Ac variants C05s, C03s, and A01s showed dramatically improved activity against Cry1Ac-resistant *T. ni*, with median lethal concentration (LC_{50}) values up to 335-fold lower than wild-type Cry1Ac (Fig. 5e and Extended Data Table 1).

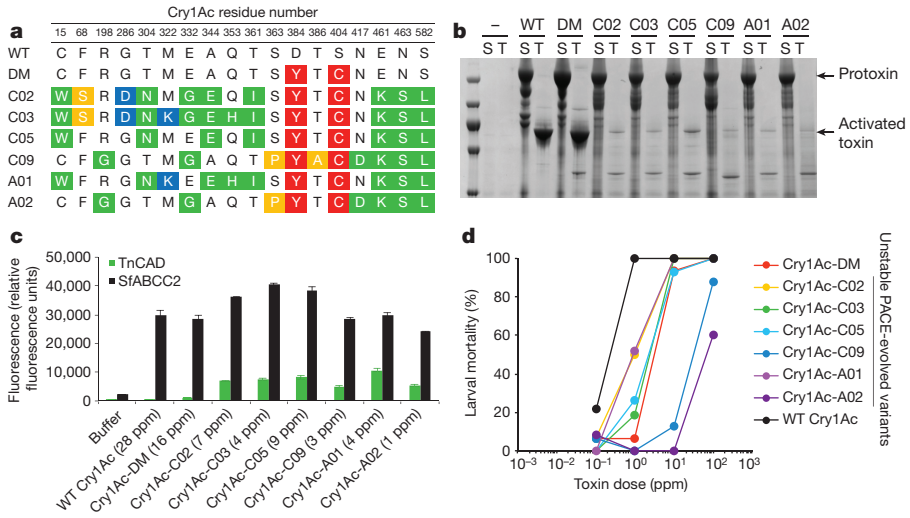

Figure 4 | Characterization of consensus-evolved Cry1Ac variants. **a**, Consensus-evolved Cry1Ac mutant sequences, including the D384Y/S404C double mutant (DM) that enabled TnTBR3-F3 recognition during the first segment of PACE. **b**, SDS–polyacrylamide gel electrophoresis (SDS–PAGE) analysis of Cry1Ac variants after trypsin digestion, revealing proteolytic instability of consensus-evolved variants. S, solubilized crude Bt crystals; T, trypsin-treated. **c**, Toxicity assays using Sf9 cells expressing the ABCC2 (black) or TnCAD receptor (green). Cells were incubated with Cry1Ac variants after trypsin digestion at the concentrations of activated toxin shown. Cry1Ac-induced cell permeabilization causes a fluorescent dye to enter cells, resulting in an increase in fluorescence. The evolved Cry1Ac variants, but not wild-type Cry1Ac, induce permeabilization of cells expressing TnCAD. Error bars, s.d. of at least three independent biological replicates. **d**, Insect larvae diet bioassays using wild-type and evolved consensus Cry1Ac variants, showing the loss of evolved Cry1Ac potency in insect larvae arising from impaired stability.

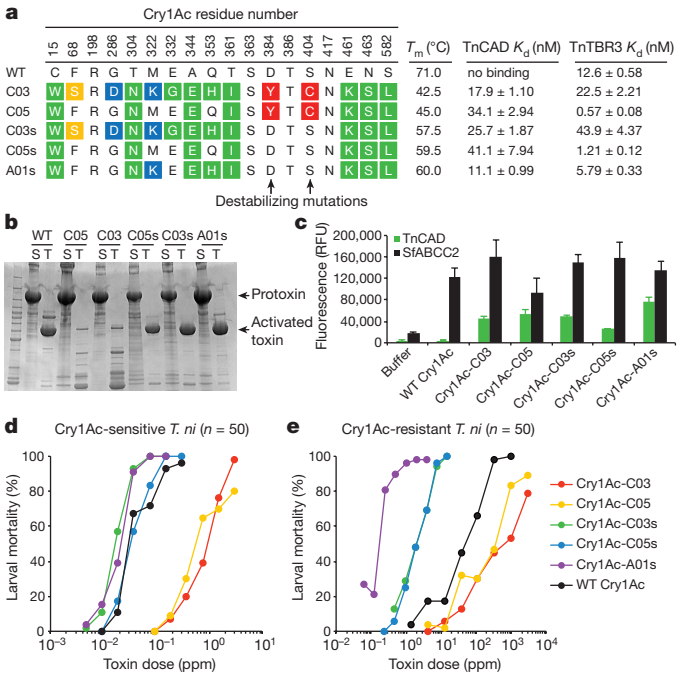

Figure 5 | Characterization of stabilized evolved Cry1Ac variants reveals potently enhanced activity. **a**, Sequence, thermal stability, and TnCAD target-binding affinity of unstable and stabilized PACE-evolved consensus mutants. **b**, SDS–PAGE analysis of trypsin digestion reactions showing dramatically enhanced stability upon D384Y and S404C reversion. **c**, Toxicity assays using Sf9 cells overexpressing the ABCC2 (black) or TnCAD receptor (green), demonstrating maintained activity of stabilized variants against both ABCC2 or TnCAD. All variants were used at 10 ppm. Error bars, s.d. of at least three independent biological replicates. **d**, **e**, Highly purified wild-type Cry1Ac, evolved consensus variants, or stabilized evolved variants were added to the diets of Cry1Ac-susceptible (**d**) or Cry1Ac-resistant (**e**) *T. ni* larvae at the indicated doses. Stabilized evolved variants moderately enhance mortality in Cry1Ac-susceptible larvae compared with wild-type Cry1Ac. Stabilized evolved variants greatly outperform wild-type Cry1Ac toxin in killing Bt toxin-resistant *T. ni* larvae.

Importantly, these evolved and stabilized Cry1Ac variants showed similar toxicity in Bt-resistant *T. ni* ($LC_{50} = 0.15$ ppm) as that of wild-type Cry1Ac in susceptible larvae ($LC_{50} = 0.04$ ppm) (Fig. 5e and Extended Data Table 1). Taken together, these results establish that the evolution of novel receptor binding among Bt toxins can overcome Bt toxin resistance in an agricultural pest.

To characterize the species profile of their insecticidal activity, we tested the evolved Cry1Ac variants in diet bioassays against 11 additional agricultural pests: a lepidopteran related to *T. ni* (*Chrysodeixis includes*, soybean looper) that encodes a cadherin-like receptor highly homologous to TnCAD, eight more distantly related lepidopteran pests, and three non-lepidopteran pests (Extended Data Figs 7 and 8). As expected, the stabilized evolved Cry1Ac variants were more potent than wild-type Cry1Ac against *C. includes*, and comparably potent as wild-type Cry1Ac against the other pests assayed (Extended Data Fig. 7). These results further support the mechanism of action of the PACE-evolved Bt toxins as binding to the cadherin receptor in *T. ni* and the closely related cadherin receptor in *C. includes*. Notably, the evolved Bt toxins did not acquire new activity against species lacking a receptor homologous to TnCAD. Taken together, these findings demonstrate that an evolved Bt toxin that binds a novel target can potently kill closely related insect pest species, while maintaining a similar overall insect spectrum as the parental Bt toxin.

Discussion

Protein-binding PACE rapidly discovered variants of Cry1Ac that bind with high affinity to the novel receptor TnCAD. Perhaps unsurprisingly, we observed a moderate reduction in stability of the evolved variants compared with wild-type Cry1Ac, as stability was not an implicit requirement of the selection. The two mutations that reduced Cry1Ac stability (D384Y and S404C) arose within the first few days of PACE on the stepping-stone target TnTBR3-F3 and were inherited by virtually all subsequent evolved variants (Fig. 3e). It is tempting to speculate that these mutations broadened the substrate scope of Cry1Ac binding to enable downstream protein evolution, at the expense of stability, but were not required once affinity for TnCAD-F3 evolved. Additional affinity measurements of reverted consensus mutations reveal the key roles of E461K, N463S, and S582L, which evolved in quick succession during the third PACE segment (Fig. 3e), consistent with their contri-

bution to TnCAD binding. All three mutations lie on the same face of Cry1Ac (Extended Data Fig. 5c), albeit in different domains, suggestive of potential direct interaction with the cadherin receptor.

Collectively, our findings establish that the laboratory evolution of novel or enhanced Bt toxin–receptor interactions can overcome insect resistance to Bt toxins. This strategy complements existing approaches to limit the incidence of Bt toxin resistance. The 'gene pyramiding' strategy for resistance management[30], for example, requires the availability of multiple effective toxins with different binding sites in target insects. The refuge strategy[4] necessitates that the resistance is a recessive trait and requires compliance by growers. The engineering of Bt toxins to eliminate the reliance on cadherin receptor interaction for toxin oligomerization has been shown to enhance toxicity against resistant strains of several insects, but also reduces the insecticidal potency of the toxins against sensitive insects[31] and may broaden the target specificity of the toxin.

The approach established here enables targeting of a Bt-resistant pest through the evolution of high-affinity Bt toxin variants that bind a specific target insect protein. In principle, this strategy should be applicable to target a variety of insect pests. While the evolution of insect resistance to an evolved Bt toxin is a likely possibility, this work has the potential to provide access to many new Bt toxins that, individually or in combination, may manage resistance and extend the effectiveness of this important approach to pest control. We also envision that this system may be used to explore potential resistance mechanisms by evolving the receptor in the presence of a Bt toxin, analogous to the recent use of PACE to identify protease inhibitor drug resistance mechanisms[10]. Finally, we note that the ability of protein-binding PACE to rapidly evolve novel protein–protein interactions may prove useful in the discovery or improvement of protein therapeutics.

Online Content Methods, along with any additional Extended Data display items and Source Data, are available in the online version of the paper; references unique to these sections appear only in the online paper.

Received 6 December 2015; accepted 23 March 2016.
Published online 27 April 2016.

1. Prado, J. R. *et al.* Genetically engineered crops: from idea to product. *Annu. Rev. Plant Biol.* **65,** 769–790 (2014).
2. Pardo-López, L., Soberón, M. & Bravo, A. *Bacillus thuringiensis* insecticidal three-domain Cry toxins: mode of action, insect resistance and consequences for crop protection. *FEMS Microbiol. Rev.* **37,** 3–22 (2013).
3. James, C. *Global Status of Commercialized Biotech/GM Crops: 2014.* ISAAA Brief No. 49 (International Service for the Acquisition of Agri-biotech Applications, 2014).
4. Tabashnik, B. E., Brévault, T. & Carrière, Y. Insect resistance to Bt crops: lessons from the first billion acres. *Nature Biotechnol.* **31,** 510–521 (2013).
5. Adang, M. J., Crickmore, N. & Jurat-Fuentes, J. L. Diversity of *Bacillus thuringiensis* crystal toxins and mechanism of action. *Adv. Insect Physiol.* **47,** 39–87 (2014).
6. Esvelt, K. M., Carlson, J. C. & Liu, D. R. A system for the continuous directed evolution of biomolecules. *Nature* **472,** 499–503 (2011).
7. Dickinson, B. C., Leconte, A. M., Allen, B., Esvelt, K. M. & Liu, D. R. Experimental interrogation of the path dependence and stochasticity of protein evolution using phage-assisted continuous evolution. *Proc. Natl Acad. Sci. USA* **110,** 9007–9012 (2013).
8. Leconte, A. M. *et al.* A population-based experimental model for protein evolution: effects of mutation rate and selection stringency on evolutionary outcomes. *Biochemistry* **52,** 1490–1499 (2013).
9. Carlson, J. C., Badran, A. H., Guggiana-Nilo, D. A. & Liu, D. R. Negative selection and stringency modulation in phage-assisted continuous evolution. *Nature Chem. Biol.* **10,** 216–222 (2014).
10. Dickinson, B. C., Packer, M. S., Badran, A. H. & Liu, D. R. A system for the continuous directed evolution of proteases rapidly reveals drug-resistance mutations. *Nature Commun.* **5,** 5352 (2014).
11. Hubbard, B. P. *et al.* Continuous directed evolution of DNA-binding proteins to improve TALEN specificity. *Nature Methods* **12,** 939–942 (2015).
12. Badran, A. H. & Liu, D. R. Development of potent *in vivo* mutagenesis plasmids with broad mutational spectra. *Nature Commun.* **6,** 8425 (2015).
13. Dove, S. L. & Hochschild, A. Conversion of the omega subunit of *Escherichia coli* RNA polymerase into a transcriptional activator or an activation target. *Genes Dev.* **12,** 745–754 (1998).
14. Wojcik, J. *et al.* A potent and highly specific FN3 monobody inhibitor of the Abl SH2 domain. *Nature Struct. Mol. Biol.* **17,** 519–527 (2010).
15. Gómez, I. *et al.* Role of receptor interaction in the mode of action of insecticidal Cry and Cyt toxins produced by *Bacillus thuringiensis*. *Peptides* **28,** 169–173 (2007).
16. Fabrick, J. A. & Tabashnik, B. E. Binding of *Bacillus thuringiensis* toxin Cry1Ac to multiple sites of cadherin in pink bollworm. *Insect Biochem. Mol. Biol.* **37,** 97–106 (2007).
17. Wu, Y. D. Detection and mechanisms of resistance evolved in insects to cry toxins from *Bacillus thuringiensis*. *Adv. Insect Physiol.* **47,** 297–342 (2014).
18. Xie, R. *et al.* Single amino acid mutations in the cadherin receptor from *Heliothis virescens* affect its toxin binding ability to Cry1A toxins. *J. Biol. Chem.* **280,** 8416–8425 (2005).
19. Hua, G., Jurat-Fuentes, J. L. & Adang, M. J. Bt-R1a extracellular cadherin repeat 12 mediates *Bacillus thuringiensis* Cry1Ab binding and cytotoxicity. *J. Biol. Chem.* **279,** 28051–28056 (2004).
20. Nagamatsu, Y., Koike, T., Sasaki, K., Yoshimoto, A. & Furukawa, Y. The cadherin-like protein is essential to specificity determination and cytotoxic action of the *Bacillus thuringiensis* insecticidal CrylAa toxin. *FEBS Lett.* **460,** 385–390 (1999).
21. Peng, D., Xu, X., Ye, W., Yu, Z. & Sun, M. *Helicoverpa armigera* cadherin fragment enhances Cry1Ac insecticidal activity by facilitating toxin-oligomer formation. *Appl. Microbiol. Biotechnol.* **85,** 1033–1040 (2010).
22. Eren, A. M. *et al.* Oligotyping: differentiating between closely related microbial taxa using 16S rRNA gene data. *Methods Ecol. Evol.* **4,** 1111–1119 (2013).
23. Chougule, N. P. *et al.* Retargeting of the *Bacillus thuringiensis* toxin Cyt2Aa against hemipteran insect pests. *Proc. Natl Acad. Sci. USA* **110,** 8465–8470 (2013).
24. Fujii, Y. *et al.* Affinity maturation of Cry1Aa toxin to the *Bombyx mori* cadherin-like receptor by directed evolution. *Mol. Biotechnol.* **54,** 888–899 (2013).
25. Tiewsiri, K. & Wang, P. Differential alteration of two aminopeptidases N associated with resistance to *Bacillus thuringiensis* toxin Cry1Ac in cabbage looper. *Proc. Natl Acad. Sci. USA* **108,** 14037–14042 (2011).
26. Baxter, S. W. *et al.* Parallel evolution of *Bacillus thuringiensis* toxin resistance in Lepidoptera. *Genetics* **189,** 675–679 (2011).
27. Zhang, X., Tiewsiri, K., Kain, W., Huang, L. & Wang, P. Resistance of *Trichoplusia ni* to *Bacillus thuringiensis* toxin Cry1Ac is independent of alteration of the cadherin-like receptor for Cry toxins. *PLoS ONE* **7,** e35991 (2012).
28. Wang, P. *et al.* Mechanism of resistance to *Bacillus thuringiensis* toxin Cry1Ac in a greenhouse population of the cabbage looper, *Trichoplusia ni*. *Appl. Environ. Microbiol.* **73,** 1199–1207 (2007).
29. Song, X., Kain, W., Cassidy, D. & Wang, P. Resistance to *Bacillus thuringiensis* toxin Cry2Ab in *Trichoplusia ni* is conferred by a novel genetic mechanism. *Appl. Environ. Microbiol.* **81,** 5184–5195 (2015).
30. Carrière, Y., Crickmore, N. & Tabashnik, B. E. Optimizing pyramided transgenic Bt crops for sustainable pest management. *Nature Biotechnol.* **33,** 161–168 (2015).
31. Tabashnik, B. E. *et al.* Efficacy of genetically modified Bt toxins against insects with different genetic mechanisms of resistance. *Nature Biotechnol.* **29,** 1128–1131 (2011).

Supplementary Information is available in the online version of the paper.

Acknowledgements This work was supported by National Institutes of Health/National Institute of Biomedical Imaging and Bioengineering R01EB022376, DARPA HR0011-11-2-0003, DARPA N66001-12-C-4207, the Howard Hughes Medical Institute, and the US Department of Agriculture National Institute of Food and Agriculture and Agricultural Research Service Biotechnology Risk Assessment Grant Program 2012-33522-19791. A.H.B. was supported by the Harvard Chemical Biology Program and a National Science Foundation Graduate Research Fellowship. We are grateful to J. Carlson, J. Nageotte, D. Rappoli, J.-L. Kouadio, M. Zheng, J. Milligan, M. Huang, Z. Du, X. Zhou, E. Kraft, and J. Wang for their assistance.

Author Contributions A.H.B. designed the research, performed experiments, analysed data, and wrote the manuscript. D.R.L. designed and supervised the research and wrote the manuscript. V.M.G. and T.M. designed the initial Cry1Ac/TBR3 pair for evolution in PACE. V.M.G. designed and supervised the research on the evaluation of evolved and stabilized Cry1Ac variants. V.M.G. and P.V. designed stabilized Cry1Ac variants. Q.H. performed protein purification and *in vitro* binding analysis, and analysed data. M.M.K. performed the insect cell-based assays. W.K., P.W., and A.M.N. performed insect diet bioassays using evolved Cry1Ac variants. A.E. and F.M. designed and validated the Cry1Ac-binding TBR3 mutant. K.H.T. analysed high-throughput sequencing data. All of the authors contributed to editing the manuscript.

Author Information Reprints and permissions information is available at www.nature.com/reprints. The authors declare competing financial interests: details are available in the online version of the paper. Readers are welcome to comment on the online version of the paper. Correspondence and requests for materials should be addressed to D.R.L. (drliu@fas.harvard.edu).

METHODS

No statistical methods were used to predetermine sample size. The *in vivo* experiments were blinded and randomized.

General methods. PCR was performed using PfuTurbo Cx Hotstart DNA polymerase (Agilent Technologies), VeraSeq ULtra DNA polymerase (Enzymatics), or Phusion U Hot Start DNA Polymerase (Life Technologies). Water was purified using a MilliQ water purification system (Millipore). Plasmids and selection phages were constructed using USER cloning (New England Biolabs). Genes were either synthesized as bacterial codon-optimized gBlocks Gene Fragments (Integrated DNA Technologies) or amplified by PCR from native sources. *Cry1ac* was amplified by PCR from the *B. thuringiensis* strain Bt_B107284 and cloned into the Bt expression vector pMON101647 using Hot Fusion[32] to generate the expression plasmid pMON133051, which served as a template for amplifying *Cry1ac* fragments for constructing PACE vectors. The toxin-binding region from *T. ni* cadherin (A1133–T1582, AEA29692.10), referred to as TnCAD-FL, was synthesized using 45–60-base oligonucleotides (Integrated DNA Technologies) by overlap extension PCR using KOD Hot Start DNA polymerase (EMD Millipore). The synthetic wild-type TnCAD-FL template was used to generate the TnTBR3-FL fragment via site-directed mutagenesis using the QuikChange II kit according to the manufacturer's instructions (Agilent Technologies). DNA vector amplification was performed using NEB Turbo or DH5α cells (New England Biolabs).

Electrocompetent strain preparation. The previously described strains S1030 (ref. 9) or S2060 (ref. 11) were used in all luciferase and plaque assays, as well as in PACE experiments. The glycerol stock of either strain was used to seed a 2-ml overnight culture using 2xYT media (United States Biological) supplemented with 10 μg ml^{-1} tetracycline (Sigma Aldrich), 50 μg ml^{-1} streptomycin (Sigma Aldrich), 10 μg ml^{-1} fluconazole (TCI America), and 10 μg ml^{-1} amphotericin B (TCI America) in a 37 °C shaker at 230 r.p.m. The saturated culture was diluted 1,000-fold in 50 ml of the same supplemented media and grown under identical conditions until it reached mid-log-phase (absorbance at 600 nm ($A_{600\,nm}$) = 0.5–0.8). Once the appropriate $A_{600\,nm}$ was reached, the cells were pelleted in a 50-ml conical tube (VWR) centrifuged at 10,000*g* for 5 min at 4 °C. The supernatant was immediately decanted and the interior of the tube was wiped with a few Kimwipes (Kimberly-Clark) to remove residual media and salts. The cells were resuspended in 25 ml of pre-chilled, sterile filtered 10% glycerol in MilliQ purified water using a pipette to quickly break up the pellet. The cells were centrifuged and washed an additional three times. After the last centrifugation step, the interior of the tube was wiped with a few Kimwipes to remove residual glycerol solution. The pellet was resuspended in as little volume as possible, typically ~150 μl, and split into 10 μl aliquots for storage. Cells were flash frozen using a liquid N_2 bath, then quickly transferred to −80 °C for extended storage. Electrocompetent S1030 or S2060 cells produced by this method typically yielded 10^7–10^8 colonies per microgram plasmid DNA and enable the simultaneous electroporation of up to three plasmids carrying orthogonal origins of replication and antibiotic resistance cassettes to yield transformants containing all plasmids.

General USER cloning. All PACE-related plasmids and phage materials were constructed via USER cloning[33] (see Extended Data Table 2). Briefly, primers were designed to include a single internal deoxyuracil base 15–20 bases from the 5′ end of the primer, specifying this region as the 'USER junction'. Criteria for design of the USER junction were: it should contain minimal secondary structure, have 45 °C < T_m < 70 °C, and begin with a deoxyadenosine and end with a deoxythymine (to be replaced by deoxyuridine). The USER junction specifies the homology required for correct assembly. We note that PfuTurbo Cx Hotstart DNA polymerase (Agilent Technologies), VeraSeq ULtra DNA polymerase (Enzymatics), or Phusion U Hot Start DNA Polymerase (Life Technologies) are able to use primers carrying deoxyuracil bases, whereas some other polymerases undergo a phenomenon known as PCR poisoning and do not extend the primer.

All PCR products were purified using a MinElute PCR Purification Kit (Qiagen) to 10 μl final volume and quantified using a NanoDrop 1000 Spectrophotometer (Thermo Scientific). For assembly, PCR products carrying complementary USER junctions were mixed in an equimolar ratio (up to 1 pmol each) in a 10 μl reaction containing 15 units DpnI (New England Biolabs), 0.75 units USER (Uracil-Specific Excision Reagent) enzyme (Endonuclease VIII and Uracil-DNA Glycosylase, NEB), 50 mM potassium acetate, 20 mM Tris-acetate, 10 mM magnesium acetate, 100 μg ml^{-1} BSA at pH 7.9 (1× CutSmart Buffer, New England Biolabs). The reactions were incubated at 37 °C for 45 min, followed by heating to 80 °C and slow cooling to 22 °C at 0.1 °C s^{-1} in a temperature-controlled block. The hybridized constructs were directly used for heat-shock transformation of chemically competent NEB Turbo *E. coli* cells according to the manufacturer's instructions. Transformants were selected on 1.8% agar-2xYT plates supplemented with the appropriate antibiotic(s).

For selection phage cloning, the hybridized constructs were purified using EconoSpin purification columns (Epoch Life Sciences), eluted using 25 μl 10% glycerol, and transformed into electrocompetent S2060 cells carrying the phage-responsive accessory plasmid pJC175e, which produces functional pIII in response to phage infection (this strain is henceforth referred to as S2208). After recovery for 3–4 h at 37 °C using 2xYT (United States Biological) media, the culture was centrifuged and the supernatant was purified using a 0.22 μm PVDF Ultrafree centrifugal filter (Millipore). The supernatant was diluted serially in 100-fold increments and used in plaque assays using log-phase S2208 cells. After overnight at 37 °C, single plaques were picked into 2xYT media and grown for 12–18 h in a 37 °C shaker at 230 r.p.m. The supernatant was purified again to yield clonal phage stocks. In all cases, cloned plasmids and phages were prepared using the TempliPhi 500 Amplification Kit (GE Life Sciences) according to the manufacturers protocol and verified by Sanger sequencing.

Plaque assays. S1030 (ref. 9) or S2060 (ref. 11) cells transformed with the accessory plasmid of interest were grown in 2xYT (United States Biological) liquid media supplemented with the appropriate antibiotics to an $A_{600\,nm}$ of 0.6–0.9. The phage supernatant was diluted serially in three, 100-fold increments to yield four total samples (undiluted, 10^2-, 10^4-, and 10^6-fold diluted) to be used for infections. For each sample, 150 μl of cells were added to 10 μl of phage that had been filtered using a 0.22 μm PVDF Ultrafree centrifugal filter (Millipore). Within 1–2 min of infection, 1 ml of warm (~55 °C) top agar (7 g l^{-1} bacteriological agar in 2xYT) was added to the phage/cell mixture, mixed by pipetting up and down once, and plated onto quartered plates that had been previously poured with 2 ml of bottom agar (18 g l^{-1} bacteriological agar in 2xYT) in each quadrant. The plates were then grown overnight at 37 °C before plaques could be observed.

PACE. Host cell cultures, lagoons, media, and the PACE apparatus were as previously described[9]. Recombined selection phage harbouring gene III (rSP) will poison a PACE experiment by outcompeting the evolving selection phage. We have noted that the likelihood of rSP occurrence in a selection phage stock increases with extended standing culture growth during the initial selection phage stock preparation. To reduce the likelihood of rSP formation, all selection phages are repurified before any continuous evolution experiments. Briefly, selection phages were plaqued on S2208 cells. A single plaque was picked into 2 ml 2xYT (United States Biological) supplemented with the appropriate antibiotics and grown until the culture reached mid-log-phase ($A_{600\,nm}$ = 0.5–0.8). The culture was centrifuged using a table-top centrifuge for 2 min at 10,000*g*, followed by supernatant filtration using a 0.22 μm PVDF Ultrafree centrifugal filter (Millipore). This short growth period routinely yields titres of 10^6–10^8 plaque-forming units per millilitre and was found to minimize the occurrence of rSP during PACE experiments.

To prepare the PACE strain, the accessory plasmid and MP were co-transformed into electrocompetent S1030 cells (see above) and recovered using Davis rich media[9] (DRM) to ensure MP repression. Transformations were plated on 1.8% agar-2xYT containing 50 μg ml^{-1} carbenicillin, 40 μg ml^{-1} chloramphenicol, 10 μg ml^{-1} fluconazole, 10 μg ml^{-1} amphotericin B, 100 mM glucose (United States Biological) and grown for 12–18 h in a 37 °C incubator. After overnight growth, four single colonies were picked and resuspended in DRM, then serially diluted and plated on 1.8% agar-2xYT containing 50 μg ml^{-1} carbenicillin, 40 μg ml^{-1} chloramphenicol, 10 μg ml^{-1} fluconazole, 10 μg ml^{-1} amphotericin B, and either 100 mM glucose or 100 mM arabinose (Gold Biotechnology) and grown for 12–18 h in a 37 °C incubator. Concomitant with this plating step, the dilution series was used to inoculate liquid cultures in DRM supplemented with 50 μg ml^{-1} carbenicillin, 40 μg ml^{-1} chloramphenicol, 10 μg ml^{-1} tetracycline, 50 μg ml^{-1} streptomycin, 10 μg ml^{-1} fluconazole, 10 μg ml^{-1} amphotericin B and grown for 12–18 h in a 37 °C shaker at 230 r.p.m. After confirmation of arabinose sensitivity using the plate assay, cultures of the serially diluted colonies still in log-phase growth were used to seed a 25-ml starter culture for the PACE chemostat.

Once the starter culture had reached log-phase density ($A_{600\,nm}$ = 0.5–0.8), the 25-ml culture was added directly to 175 ml of fresh DRM in the chemostat. The chemostat culture was maintained at 200 ml and grown at a dilution rate of 1.5–1.6 volumes per hour as previously described[9]. Lagoons flowing from the chemostats were maintained at 40 ml, and diluted as described for each experiment. Lagoons were supplemented with 25 mM arabinose to induce the MP for 8–16 h before infection with packaged selection phage. Samples were taken at the indicated time points, centrifuged at 10,000*g* for 2 min, then filtered with a 0.2 μm filter and stored overnight at 4 °C. Phage aliquots were titred by plaque assay on S2208 cells (total phage titre) and S1030 or S2060 cells (rSP titre) for all time points.

Mutagenesis during PACE. The basal mutation rate of replicating filamentous phage in *E. coli* (7.2×10^{-7} substitutions per base pair per generation) is sufficient to generate all possible single but not double mutants of a given gene in a 40-ml lagoon after one generation of phage replication. For the 2,139-base-pair *rpoZ–Cry1Ac* target, a basal mutation rate of 7.2×10^{-7} substitutions per base pair per generation applied to 2×10^{10} copies of the gene (a single generation)

in a 40-ml lagoon yields $\sim 3.1 \times 10^7$ base substitutions, easily enough to cover all 6,417 single point mutants but not all double mutants. Arabinose induction of our first-generation mutagenesis plasmid, MP1, increased the phage mutation rate by ~100-fold, resulting in 7.2×10^{-5} substitutions per base pair per generation, yielding $\sim 3.1 \times 10^9$ substitutions spread over 2×10^{10} copies of the gene after a single generation. This enhanced mutation rate is sufficient to cover all possible single mutants (6.4×10^3 possibilities) and double mutants (4.1×10^7 possibilities), but no triple mutants (2.6×10^{11} possibilities) after a single phage generation. Our recent efforts to enhance mutagenesis in PACE yielded the improved MP6 system[12], which increases the phage mutation rate by an additional 100-fold compared with MP1, resulting in 7.2×10^{-3} substitutions per base pair per generation, yielding $\sim 3.1 \times 10^{11}$ substitutions spread over 2×10^{10} copies of the gene after a single generation. This elevated mutation rate is sufficient to cover all possible single mutants (6.4×10^3 possibilities), double mutants (4.1×10^7 possibilities), and many triple mutants (2.6×10^{11} possibilities) after a single phage generation.

Luciferase assays. Complementary plasmids were co-transformed with an accessory plasmid of interest into electrocompetent S1030 (ref. 9) or S2060 (ref. 11) cells and plated onto 1.8% agar-2xYT plates with 50 μg ml^{-1} carbenicillin and 100 μg ml^{-1} spectinomycin. After overnight growth at 37 °C, single colonies were each picked into 2 ml DRM supplemented with 50 μg ml^{-1} carbenicillin, 100 μg ml^{-1} spectinomycin, 10 μg ml^{-1} tetracycline, 50 μg ml^{-1} streptomycin, 10 μg ml^{-1} fluconazole, 10 μg ml^{-1} amphotericin B and grown for 12–18 h in a 37 °C shaker at 230 r.p.m. After overnight growth, cultures were diluted 1,000-fold in a 96-well deep well plate containing 500 μl DRM with 50 μg ml^{-1} carbenicillin, 100 μg ml^{-1} spectinomycin, and the indicated arabinose, isopropyl-β-D-thiogalactoside (IPTG), or anhydrotetracycline (ATc) concentration to induce protein expression from either the accessory plasmid or complementary plasmid. Constitutive accessory plasmids and complementary plasmids were used where no inducer concentration is given. After growth with shaking at 37 °C for 4–5 h, 150 μl of each culture was transferred to a 96-well black wall, clear bottom plate (Costar), and the $A_{600\,nm}$ and luminescence for each well was measured on an Infinite M1000 Pro microplate reader (Tecan). The $A_{600\,nm}$ of a well containing only media was subtracted from all sample wells to obtain a corrected $A_{600\,nm}$ value for each well. The raw luminescence value for each well was then divided by that well's corrected $A_{600\,nm}$ value to obtain the luminescence value normalized to cell density. Each variant was assayed in at least biological triplicate, and the error bars shown reflect the standard deviations of the independent measurements.

High-throughput sequencing and oligotype analysis. Raw reads have been deposited in the NCBI Sequence Read Archive under accession number PRJNA293870, and all custom scripts used in analysis are available at http://github.com/MonsantoCo/BadranEtAl2015. Illumina reads obtained from each time point were mapped to the SP055-rpoZ-cMyc-Cry1Ac1-d123 reference sequence using bowtie version 2.1.0 (ref. 34), and the resulting SAM files were combined into a single BAM file using samtools version 0.1.19 (ref. 35). This BAM file was used as input to freebayes version 0.9.21-12-g92eb53a[36] to call single nucleotide polymorphisms, using the command 'freebayes–use-best-n-alleles 1–pooled-continuous–use-reference-allele–theta 500000000–min-alternate-fraction 0.01–ploidy 1–region SP055-rpoZ-cMyc-Cry1Ac1-d123:2833-4971'. The analysis is encapsulated in the custom script 'ill.callsnps.sh.' PacBio polymerase reads were demultiplexed with RS_Resequencing_Barcode.1 workflow provided by PacBio. Polymerase reads with quality score lower than 0.80 (defined by the PacBio scoring algorithm) or shorter than 50 base pairs were filtered. High-quality reads were processed into subreads after sequencing primers and adaptors were removed. Circular consensus reads (or reads-of-inserts) were obtained by calling consensus of subreads generated from the same polymerase reads. These circular consensus reads were mapped to the SP055-rpoZ-cMyc-Cry1Ac1-d123 reference sequence using BLASR version 1.3.1.142244 (ref. 37), and the alignment was exported as an aligned FASTA sequence using the custom script 'SAMtoAFA.py.' The aligned FASTA was used as input to the oligotyping platform[22], manually specifying entropy components as the positions at which the Illumina data defined informative single nucleotide polymorphisms. Only oligotypes that occur at >1% in at least one sample were retained. This methodology resulted in informative changes at 25 of the 27 specified components. Oligotypes with gaps at the specified components, probably because of indels in the PacBio sequencing or alignment, were reassigned to other oligotypes with nucleotides in those positions only when it could be done unambiguously, and discarded otherwise, resulting in a total fraction abundance <1 in Fig. 5d. The resulting oligotype-percent abundance matrix was read into R and analysed using the custom script 'PedigreeAndMullerPlot.R.' The pedigree was refined manually, assuming that single-mutant derivatives of previous oligotypes were due to *de novo* mutation, while double, triple, or greater mutations that can be explained by recombination of previously observed oligotypes were due to recombination, since these last types of mutation were highly unlikely to arise by multiple point mutation after the start of the PACE experiment.

High-throughput primary Bt toxin preparation and analysis. Wild-type *Cry1Ac* was cloned into the Bt expression vector pMON262346 using BspQ1 endonuclease restriction sites. Consensus PACE-evolved *Cry1Ac* variants were synthesized (Gen9) and cloned into the Bt expression vector pMON262346 using Hot Fusion[32]. Reversion mutants of consensus Cry1Ac PACE variants were generated via PCR with Phusion High-Fidelity DNA polymerase (New England Biolabs) and mutant primers followed by Hot Fusion into the Bt expression vector pMON262346. The resulting plasmids were transformed into the protease-deficient Bt strain EG10650 (ref. 38) for protein expression. Cells were grown from single colonies in 96-well plates (Thermo Scientific, AB-0932) overnight in 400 μl Brain Heart Infusion Glycerol (BHIG) media (VWR) supplemented with 5 μg ml^{-1} chloramphenicol. Overnight cultures were used to prepare glycerol stocks (15% glycerol final concentration) and stored at −80 °C for future protein expression. After overnight growth, 10 μl of each culture was used to inoculate 1 ml of complete *C2* medium[39] containing 5 μg ml^{-1} chloramphenicol in 96-well plates. The plates were incubated at 26 °C with vigorous shaking at 550 r.p.m. in a Multitron shaking incubator (Infors HT) for 72 h. The cells were harvested by centrifugation at 3,200*g* for 15 min at 4 °C. The supernatant was decanted and a single 3.5 mm glass bead was added to each well of the plate. The pellet was then resuspended in 1 ml of TX wash buffer composed of 10 mM Tris-HCl, pH 7.5, 0.005% Triton X-100 supplemented with 25 units per millilitre Benzonase (EMD Millipore), and 2 mM $MgCl_2$, incubated at room temperature (21 °C) for 30–60 min (with vigorous vortexing every 10 min), then centrifuged at 3,200*g* for 15 min at 4 °C. The resulting pellet was resuspended and centrifuged under identical conditions two additional times.

The washed spore/crystal pellet from each 1-ml culture was solubilized in the 96-well plate using 300 μl of solubilization buffer composed of 50 mM CAPS, pH 11, and 10 mM DTT, then incubated while shaking at room temperature (21 °C) for 1 h. The insoluble debris was pelleted by centrifugation at 3,200*g* for 15 min at 4 °C, and 200 μl of the supernatant were transferred to a sterile U-bottom 96-well plate. To each well, 10 μl of 0.2 mg ml^{-1} trypsin in 1 M Tris-HCl, pH 7.5 was added. The mixture was incubated at 37 °C for 2 h while shaking at 150 r.p.m., followed by quenching using 2 μl 0.1 M PMSF. The solution was filtered using a Millipore multiscreen plate with a 0.22 μm membrane. Protein stability was assessed by SDS–PAGE and quantified using spot densitometry. Proteins purified using this protocol were tested in downstream insect cell assays.

Secondary Bt toxin purification and analysis. Bt glycerol stocks described above were used for large-scale protein expression and purification. A 2-ml starter culture of BHIG medium supplemented with 5 μg ml^{-1} chloramphenicol was inoculated from the glycerol stocks and grown overnight at 280 r.p.m. in a 28 °C shaker. The following day, the saturated culture was transferred into 500 ml complete C2 medium containing 5 μg ml^{-1} chloramphenicol in a 2 l baffled flask and grown for an additional 72 h at 26 °C while shaking at 280 r.p.m. Sporulation and crystal formation in the culture was verified by optical microscopy of a 2-μl aliquot of the saturated Bt culture. Upon confirmation of crystals, the partly lysed sporulated cells were harvested by centrifugation at 10,000*g* for 12 min at 4 °C. The pellet was then resuspended in 100 ml TX wash buffer composed of 10 mM Tris-HCl, pH 7.5, and 0.005% Triton X-100 supplemented with 0.1 mM PMSF, 25 units per millilitre Benzonase (Sigma-Aldrich), and 2 mM $MgCl_2$, incubated at room temperature (21 °C) for 30–60 min (with vigorous vortexing every 10 min), then centrifuged at 3,200*g* for 15 min at 4 °C. The resulting pellet was resuspended and centrifuged under identical conditions two additional times.

The washed spore/crystal pellet was solubilized in 120 ml 50 mM CAPS, pH 11, 10 mM DTT at room temperature for 1 h while shaking at 130 r.p.m. The solubilized protein was separated from the insoluble debris by centrifugation at 35,000*g* for 20 min at 4 °C. The supernatant was transferred to a fresh flask, and then supplemented with 10 ml 0.2 mg ml^{-1} trypsin in 1 M Tris-HCl at pH 7.5. The mixture was incubated at 30 °C for 2–6 h with shaking at 150 r.p.m. and trypsinization was monitored by SDS–PAGE. Once the trypsin digestion reaction was complete, the mixture was centrifuged at 3,200*g* for 15 min at 4 °C. The clear supernatant was removed and mixed with PMSF to 1 mM final concentration. The sample was loaded on a 5–10 ml Q-Sepharose (GE Healthcare) anion exchange column at a flow-rate of 4 ml min^{-1} and the trypsin resistant core of the toxin was eluted in 25 mM sodium carbonate, pH 9 supplemented with 200–400 mM NaCl. Fractions containing the toxin tryptic cores were pooled, concentrated (Millipore Amicon Ultra-15 centrifugal filter Units, Fisher), and loaded on a Hiload Superdex 200 gel filtration column using an ÄKTA chromatography system (GE Healthcare). The column was pre-equilibrated and run with 25 mM sodium carbonate at pH 10.5 supplemented with 1 mM β-mercaptoethanol. Only the monomer peak of the toxin fractions was collected in each case and concentrated to 1–3 mg ml^{-1}. The final protein concentration was quantified by spot densitometry. The quality of the trypsinized toxin was assessed using the peptide mass fingerprinting method that was based on in-gel digestion of proteins by trypsin and mass spectrometry analysis of the resulted peptides.

***T. ni* receptor fragment expression and purification.** Custom expression vectors pMON251427 and IS0008 (the same as pMON251427 but with wild-type TnCAD) were used to express 6xHis-TnTBR3-FL and 6xHis-TnCAD-FL fragments in *E. coli*. Both vectors contain an amino (N)-terminal MBP-TVMV protease cleavage site tag[40] and a carboxy (C)-terminal 6× histidine tag flanking the receptor fragment of interest, with the open reading frame driven by the T7 promoter. Expression vectors were transformed into commercial BL21 (λDE3) competent cells (Life Technologies) that had been previously transformed with TVMV protease expression vector (pMON101695; encodes constitutive TVMV protease from a pACYC184 (New England Biolabs) backbone). A single colony was inoculated in 2 ml of Luria-Bertani (LB) media supplemented with 50 μg ml^{-1} kanamycin and 25 μg ml^{-1} chloramphenicol, and grown at 37 °C for 4 h to generate a starter culture, which was used to prepare glycerol stocks and stored at −80 °C for the future protein expression. A second starter culture was inoculated using the BL21 (λDE3) strain glycerol stocks in 2 ml of LB media supplemented with 50 μg ml^{-1} kanamycin and 25 μg ml^{-1} chloramphenicol and grown in a 25 °C shaker (280 r.p.m.) for 15 h. The culture was transferred into 500 ml of Terrific Broth medium (24 g l^{-1} yeast extract, 12 g l^{-1} tryptone, and 5 g l^{-1} glucose) supplemented with 50 μg ml^{-1} kanamycin and 25 μg ml^{-1} chloramphenicol, and grown at 37 °C for 4 h at 280 r.p.m., then transferred to 15 °C and grown for an additional 48 h after supplementation with IPTG to a final concentration of 0.1 mM.

The cells were harvested by centrifugation at 10,000*g* for 12 min at 4 °C. The bacterial cell pellet was resuspended in affinity buffer A (25 mM Tris-HCl at pH 8.0, 0.5 M NaCl, 15 mM imidazole, and 0.2 mM $CaCl_2$) containing 125 units per millilitre of Benzonase (EMD Millipore), 10,000 units per millilitre of chicken egg white lysozyme (Sigma Aldrich) and 1× BugBuster (Novagen). The cell slurry was incubated at room temperature for 15 min, followed by sonication using a Cell Disruptor W-0375 (Heat Systems-Ultrasonics) at 45% Duty Cycle (output number 5) for 30 s with 60 s rests for a total of three cycles. The cell lysate was centrifuged at 35,000*g* for 20 min at 4 °C. The supernatant was loaded onto a 5-ml Ni-NTA column that had been pre-equilibrated using affinity buffer A. After extensive washing with affinity buffer A, the receptor fragment was eluted with the affinity buffer B (25 mM Tris-HCl at pH 8.0, 0.1 M NaCl, 250 mM imidazole, 0.2 mM $CaCl_2$). Fractions containing the receptor fragment were pooled, concentrated and loaded on a Hiload Superdex 200 gel filtration column using an ÄKTA chromatography system (GE Healthcare). The column was pre-equilibrated and run with 25 mM Tris-HCl at pH 8.0, 0.1 M NaCl, 0.2 mM $CaCl_2$. Dimer and monomer peaks of the *T. ni* TBR3 and CAD fractions were collected separately and concentrated to 1–2 mg ml^{-1}. Only TnTBR3 and TnCAD monomers were used for Cry1Ac1 binding studies.

Fluorescence thermal shift assays. All assays were performed using a BioRad CFX96 real-time PCR thermal cycler, enabling thermal manipulations and dye fluorescence detection. The fluorescence sensitive dye SYPRO orange (Life Technologies, S6650) was used at a 5× concentration in all assays. The temperature was increased by 0.5 °C each cycle over a temperature range of 25−90 °C. Assay reactions were performed in 96-well white PCR plates (Bio-Rad, number HSP9631), and heat-sealed (Thermo Scientific, number ALPS3000) to reduce volume loss through evaporation. The data were analysed using the CFX manager software.

Protein–protein interaction affinity measurement. The Octet^{Qk} (ForteBio) and the Dip and Read Ni-NTA (NTA) biosensors were used to measure the affinity of Cry1Ac and its variants to immobilized 6xHis-TnCAD-FL or TnTBR3-FL receptor fragments in 25 mM Tris-HCl at pH 8.5, 0.1 M NaCl, 0.1 mg ml^{-1} BSA, 0.05% Tween 20 according to the manufacturer's instructions. Octet Data Acquisition 7.1.0.100 software was used for data acquisition, and ForteBio Data Analysis 7 software was used for data analysis. At least four readings at different Cry1Ac1 concentrations (2–100 nM) were used for each receptor fragment–Bt toxin interaction and a global fit was used to calculate binding affinities.

Insect cell assays. Sf9 cells (Life Technologies) were plated in Sf-900 III SFM (Life Technologies) at a density of 50,000 cells per well in a 96-well optical bottom black plate (Nunc, Thermo Scientific). The cells were incubated at 27 °C overnight to allow for adherence to the plate, and confirmed to be free of mycoplasma contamination using a MycoAlert™ Mycoplasma Detection Kit (Lonza). After overnight incubation, the medium was aspirated from the cells and 100 μl of p3 or p4 generation (third or fourth generation of baculovirus amplification in Sf9 cells after initial transfection with plasmid) recombinant baculovirus encoding each receptor diluted in SFM was added to each well. The plates were kept in a humidified environment to prevent evaporation and incubated at 27 °C for 48 h. Receptor expression was confirmed by western blotting. Toxins were diluted to the same protein concentration in 25 mM sodium carbonate at pH 11, supplemented with 1 mM β-mercaptoethanol, followed by an additional tenfold dilution in unsupplemented Grace's insect media with 2 μM SYTOX green nucleic acid stain (Life Technologies, S7020). The media was removed from the wells without disturbing the attached cells, and the diluted toxins or buffer controls were added to respective wells. The fluorescence was measured on a CLARIOstar microplate reader (BMG Labtech) after incubation for 4 h. The fluorescence intensity of control cells expressing β-glucuronidase (GUS) was subtracted from wells expressing the variable receptor fragments with or without toxins. Replicates were averaged and signal was plotted for each toxin condition.

Primary insect diet bioassays. Insect diet bioassays using the evolved consensus Cry1Ac variants were performed as previously described[41]. Briefly, 200 ml of artificial diet in 96-well plates were overlaid with 20 ml aliquots of toxin Bt spore/crystal or Bt crystal suspension, dried, after which wells were infested with neonate insect eggs suspended in 0.2% agar, dried again, sealed with Mylar sheets, and incubated at 20 °C, 60% relative humidity, in complete darkness for 5 days. The plates were scored on day 5 for larval mortality and growth stunting. Each assay was performed in three independent biological replicates with eight insects per replicate.

Secondary insect diet bioassays. An inbred Bt-susceptible laboratory strain of *T. ni* (designated the Cornell strain)[42], and a Cry1Ac-resistant strain nearly isogenic to the Cornell strain, GLEN-Cry1Ac-BCS[28], were maintained on a wheat germ-based artificial diet at 27 °C with 50% humidity and a photoperiod of 16 h light and 8 h dark[42]. Diet surface overlay bioassays were conducted to determine the insecticidal activity of the toxins in the susceptible and Cry1Ac-resistant *T. ni*, as previously described[42]. Briefly, 200 μl of each toxin dose solution was spread on the surface of 5 ml of artificial diet in 30-ml plastic rearing cups (diet surface area was ∼7 cm^2), and ten randomly selected neonatal larvae were placed into each rearing cup after the toxin solution had dried. For each bioassay, seven to eight concentrations of the toxin were used and each treatment included five replicates (50 larvae in total per concentration). Larval growth inhibition (neonates that did not reach second instar after 4 days) and mortality were recorded after 4 days of feeding. The observed larval growth inhibition and mortality were corrected using Abbott's formula[43]. Median inhibitory concentration (IC_{50}) and LC_{50} values and their 95% confidence intervals were calculated by probit analysis using the computer program POLO (LeOra Software).

32. Fu, C., Donovan, W. P., Shikapwashya-Hasser, O., Ye, X. & Cole, R. H. Hot Fusion: an efficient method to clone multiple DNA fragments as well as inverted repeats without ligase. *PLoS ONE* **9,** e115318 (2014).
33. Lund, A. M. *et al.* A versatile system for USER cloning-based assembly of expression vectors for mammalian cell engineering. *PLoS ONE* **9,** e96693 (2014).
34. Langmead, B. & Salzberg, S. L. Fast gapped-read alignment with Bowtie 2. *Nature Methods* **9,** 357–359 (2012).
35. Li, H. *et al.* The Sequence Alignment/Map format and SAMtools. *Bioinformatics* **25,** 2078–2079 (2009).
36. Garrison, E. & Marth, G. Haplotype-based variant detection from short-read sequencing. Preprint at http://adsabs.harvard.edu/abs/2012arXiv1207.3907G%3E (2012).
37. Chaisson, M. J. & Tesler, G. Mapping single molecule sequencing reads using basic local alignment with successive refinement (BLASR): application and theory. *BMC Bioinformatics* **13,** 238 (2012).
38. Tan, Y. & Donovan, W. P. Deletion of aprA and nprA genes for alkaline protease A and neutral protease A from *Bacillus thuringiensis*: effect on insecticidal crystal proteins. *J. Biotechnol.* **84,** 67–72 (2001).
39. Donovan, W. P. *et al.* Amino acid sequence and entomocidal activity of the P2 crystal protein. An insect toxin from *Bacillus thuringiensis* var. kurstaki. *J. Biol. Chem.* **263,** 561–567 (1988).
40. Nallamsetty, S. *et al.* Efficient site-specific processing of fusion proteins by tobacco vein mottling virus protease in vivo and in vitro. *Protein Expr. Purif.* **38,** 108–115 (2004).
41. Baum, J. A. *et al.* Cotton plants expressing a hemipteran-active *Bacillus thuringiensis* crystal protein impact the development and survival of *Lygus hesperus* (Hemiptera: Miridae) nymphs. *J. Econ. Entomol.* **105,** 616–624 (2012).
42. Kain, W. C. *et al.* Inheritance of resistance to *Bacillus thuringiensis* Cry1Ac toxin in a greenhouse-derived strain of cabbage looper (Lepidoptera: Noctuidae). *J. Econ. Entomol.* **97,** 2073–2078 (2004).
43. Abbott, W. S. A method of computing the effectiveness of an insecticide. 1925. *J. Am. Mosq. Control Assoc.* **3,** 302–303 (1987).

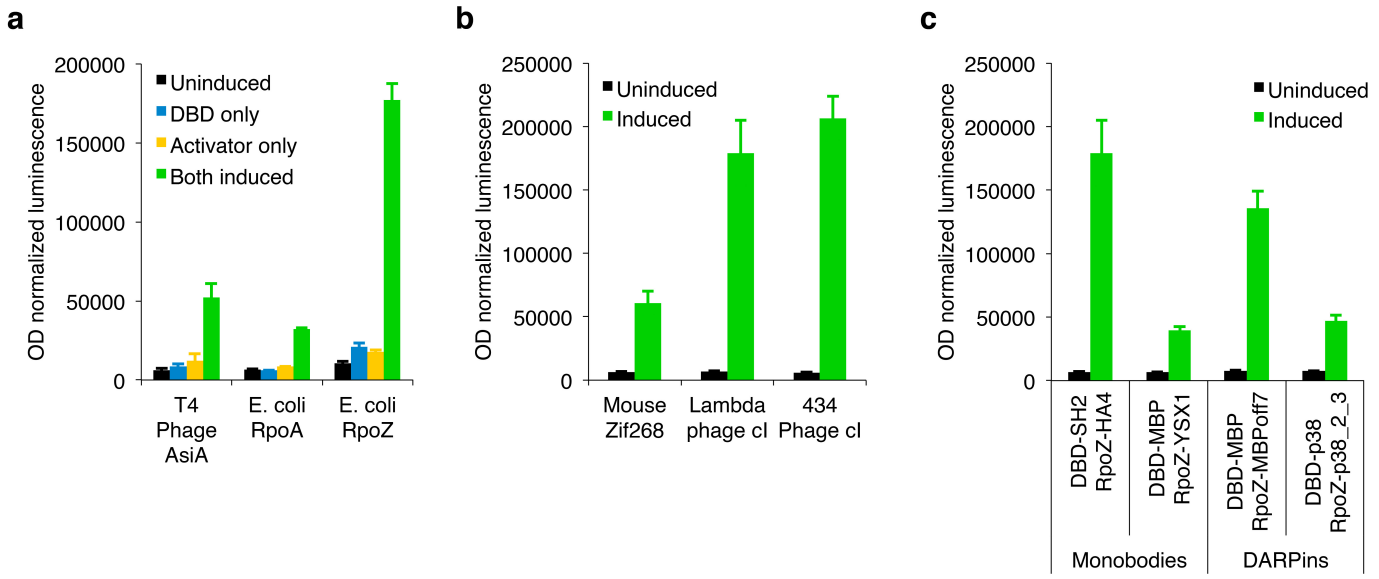

Extended Data Figure 1 | Bacterial two-hybrid component validation and optimization. a, Plasmids encoding an IPTG-inducible *λcI–SH2* cassette ('DBD') and an ATc-inducible activator-HA4 cassette ('activator') were co-transformed into the *E. coli* S1030 host strain and induced using either or both small molecules. T4 AsiA-mediated transcriptional activation required low-level expression of the σ70 (R541C/F563Y/L607P) mutant to alleviate AsiA toxicity. Use of RpoZ as the activation domain showed the greatest degree of transcriptional activation (~17-fold). **b**, DNA-binding domain variation shows that multivalent phage repressors yield a greater degree of transcriptional activation than the monomeric zinc finger Zif268. **c**, Transcriptional activation from a combination of the λcI DNA binding domain and RpoZ transcriptional activator was evaluated using several previously evolved protein–protein interactions involving either monobodies or DARPins, showing the generality of binding interaction detection. Error bars, s.d. of at least three independent biological replicates.

a

DBD	Activator	Promoter	Uninduced	Induced	Fold
Lambda cI	RpoZ	cattaggcaccccgggctttacactttatgcttccggctcgtatgttgtgtcgaccg	525	11689	22
434 cI	RpoZ	cattaggcaccccgggctttacactttatgcttccggctcgtatgttgtgtcgaccg	330	18167	55
434 cI	RpoZ	cattaggcaccccgggctttacacGtAatgcttccggcGcgtatgttgtgtcgaccg	3252	182235	56
434 cI	RpoZ	cattaggcaccccgggctttacacGtAatgcttccggcGcgtatgGtgtgtcgaccg	4542	467340	103
434 cI	RpoZ	cattaggcaccccgggctttacacGtAatgcttccggcGcgtaCgttgtgtcgaccg	767	51636	67
434 cI	RpoZ	cattaggcaccccgggctttacacGtAatgcttccggcGcgtaCgGtgtgtcgaccg	945	64088	68
434 cI	RpoZ	cattaggcaccccgggcttGacacGtAatgcttccggcGcgtatgttgtgtcgaccg	432159	712599	2
434 cI	RpoZ	cattaggcaccccgggcttGacacGtAatgcttccggcGcgtatgGtgtgtcgaccg	556230	750804	1
434 cI	RpoZ	cattaggcaccccgggctttacGcGtAatgcttccggcGcgtatgttgtgtcgaccg	1015	97100	96
434 cI	RpoZ	cattaggcaccccgggctGtacGcGtAatgcttccggcGcgtatgttgtgtcgaccg	103	8579	83
434 cI	RpoZ	cattaggcaccccgggctGtacGcGtAatgcttccggcGcgtaCgttgtgtcgaccg	69	899	13
434 cI	RpoZ	cattaggcaccccgggctGtacGcGtAatgcttccggcGcgtaCgGtgtgtcgaccg	52	678	13
434 cI	RpoZ	cattaggcaccccgggctGtacGcGtAatgcttccggcGcgtatgttgCgtcgaccg	202	1280	6
434 cI	RpoZ	cattaggcaccccgggctGtacGcGtAatgcttccggcGcgtatgttgGgtcgaccg	139	2307	17
434 cI	RpoZ	cattaggcaccccgggcttGacGcGtAatgcttccggcGcgtatgttgtgtcgaccg	50526	494779	10
434 cI	RpoZ	cattaggcaccccgggcttGacGcGtAatgcttccggcGcgtatgGtgtgtcgaccg	66275	481567	7
434 cI	RpoZ	cattaggcaccccgggcGttacacGtAatgcttccggcGcgtatgGtgtgtcgaccg	229	1851	8
434 cI	RpoZ	cattaggcaccccgggcAttacacGtAatgcttccggcGcgtatgGtgtgtcgaccg	382	3450	9
434 cI	RpoZ	cattaggcaccccgggcCttacacGtAatgcttccggcGcgtatgGtgtgtcgaccg	131	3062	23
434 cI	RpoZ	cattaggcaccccgggctGtacacGtAatgcttccggcGcgtatgGtgtgtcgaccg	725	76430	105
434 cI	RpoZ	cattaggcaccccgggctCtacacGtAatgcttccggcGcgtatgGtgtgtcgaccg	80	668	8
434 cI	RpoZ	cattaggcaccccgggctttacacGtAatgcttccggcGcgtatgttgCgtcgaccg	859	86407	101
434 cI	RpoZ	cattaggcaccccgggctttacacGtAatgcttccggcGcgtatgttgCgtcgaccg	943	97337	103
434 cI	RpoZ	cattaggcaccccgggctttacacGtAatgcttccggcGcgtatgttgCgCcgaccg	554	21807	39
434 cI	RpoZ	cattaggcaccccgggctttacacGtAatgcttccggcGcgtatgttgCgGcgaccg	428	34919	82
434 cI	RpoZ	cattaggcaccccgggctttacacGtAatgcttccggcGcgtatgttgGgtcgaccg	2229	309795	139
434 cI	RpoZ	cattaggcaccccgggctttacacGtAatgcttccggcGcgtatgttgGgCcgaccg	989	92428	93
434 cI	RpoZ	cattaggcaccccgggctttacacGtAatgcttccggcGcgtatgttgGgGcgaccg	1523	149661	98
434 cI	RpoZ	cattaggcaccccgggctttacacGtAatgcttccggcGcgtatgttgAgtcgaccg	2203	296387	135
434 cI	RpoZ	cattaggcaccccgggctttacacGtAatgcttccggcGcgtatgttgAgCcgaccg	1271	167091	131
434 cI	RpoZ	cattaggcaccccgggctttacacGtAatgcttccggcGcgtatgttgAgGcgaccg	1906	189337	99
434 cI	RpoZ	cattaggcaccccgggctttacGcGtAatgcttccggcGcgtatgttgAgCcgaccg	230	28708	125
434 cI	RpoZ	cattaggcaccccgggctttacGcGtAatgcttccggcGcgtatgttgAgGcgaccg	269	42314	158
434 cI	RpoZ	cattaggcaccccgggctGtacacGtAatgcttccggcGcgtatgttgAgCcgaccg	122	10658	87
434 cI	RpoZ	cattaggcaccccgggctGtacacGtAatgcttccggcGcgtatgttgAgGcgaccg	201	22016	109
434 cI	RpoZ	cattaggcaccccgggctttacGcGtAatgcttccggcGcgtatgGtgAgCcgaccg	566	24652	44
434 cI	RpoZ	cattaggcaccccgggctttacGcGtAatgcttccggcGcgtatgGtgAgGcgaccg	753	78485	104
434 cI	RpoZ	cattaggcaccccgggctGtacacGtAatgcttccggcGcgtatgGtgAgCcgaccg	878	26019	30
434 cI	RpoZ	cattaggcaccccgggctGtacacGtAatgcttccggcGcgtatgGtgAgGcgaccg	1041	52307	50
434 cI	RpoZ	cattaggcaccccgggAtttacacGtAatgcttccggcGcgtatgttgtgtcgaccg	2480	164725	66
434 cI	RpoZ	cattaggcaccccgggctttGcacGtAatgcttccggcGcgtatgttgtgtcgaccg	1015	46198	46
434 cI	RpoZ	cattaggcaccccgggctttacTcGtAatgcttccggcGcgtatgttgtgtcgaccg	1294	151683	117
434 cI	RpoZ	cattaggcaccccgggctttacTcGtCatgcttccggcGcgtatgttgtgtcgaccg	1259	134645	107
434 cI	RpoZ	cattaggcaccccgggctttacTcGtAaAgcttccggcGcgtatgttgtgtcgaccg	412	80809	196
434 cI	RpoZ	cattaggcaccccgggctttacTcGtAatgcttccggTGcgtatgttgtgtcgaccg	613	38195	62
434 cI	RpoZ	cattaggcaccccgggctttacCcGtAatgcttccggcGcgtatgttgtgtcgaccg	601	53127	88
434 cI	RpoZ	cattaggcaccccgggctttacacGtCatgcttccggcGcgtatgttgtgtcgaccg	2975	371487	125
434 cI	RpoZ	cattaggcaccccgggctttacacGtCaAgcttccggcGcgtatgttgtgtcgaccg	1903	255198	134
434 cI	RpoZ	cattaggcaccccgggctttacacGtCatgcttccggTGcgtatgttgtgtcgaccg	1271	2597	2
434 cI	RpoZ	cattaggcaccccgggctttacacGtAaAgcttccggcGcgtatgttgtgtcgaccg	1371	218447	159
434 cI	RpoZ	cattaggcaccccgggctttacacGtAaAgcttccggTGcgtatgttgtgtcgaccg	813	62941	77
434 cI	RpoZ	cattaggcaccccgggctttacacGtAatgcCtccggcGcgtatgttgtgtcgaccg	33730	218546	6
434 cI	RpoZ	cattaggcaccccgggctttacacGtAatgcttccggTGcgtatgttgtgtcgaccg	1146	160609	140
434 cI	RpoZ	cattaggcaccccgggctttacacGtAatgcttccggcGTgtatgttgtgtcgaccg	39981	777784	19
434 cI	RpoZ	cattaggcaccccgggctttacacGtAatgcttccggcGAgtatgttgtgtcgaccg	6010	638749	106
434 cI	RpoZ	cattaggcaccccgggctttacacGtAatgcttccggcGcgtaGgttgtgtcgaccg	489	46068	94
434 cI	RpoZ	cattaggcaccccgggctttacacGtAatgcttccggcGcgtatgtAgtgtcgaccg	291	4553	16
434 cI	RpoZ	cattaggcaccccgggctttacTcGtAatgcttccggcGcgtatgttgAgCcgaccg	685	44500	65
434 cI	RpoZ	cattaggcaccccgggctttacTcGtCatgcttccggcGcgtatgttgAgCcgaccg	638	43688	68
434 cI	RpoZ	cattaggcaccccgggctttacTcGtAaAgcttccggcGcgtatgttgAgCcgaccg	488	18713	38
434 cI	RpoZ	cattaggcaccccgggctttacTcGtAatgcttccggTGcgtatgttgAgCcgaccg	278	9431	34
434 cI	RpoZ	cattaggcaccccgggctttacacGtCatgcttccggcGcgtatgttgAgCcgaccg	1890	176933	94
434 cI	RpoZ	cattaggcaccccgggctttacacGtCaAgcttccggcGcgtatgttgAgCcgaccg	709	68843	97
434 cI	RpoZ	cattaggcaccccgggctttacacGtCatgcttccggTGcgtatgttgAgCcgaccg	908	49205	54
434 cI	RpoZ	cattaggcaccccgggctttacacGtAaAgcttccggcGcgtatgttgAgCcgaccg	1060	70184	66
434 cI	RpoZ	cattaggcaccccgggctttacacGtAaAgcttccggTGcgtatgttgAgCcgaccg	524	17228	33
434 cI	RpoZ	cattaggcaccccgggctttacacGtAatgcttccggTGcgtatgttgAgCcgaccg	696	36530	52

b

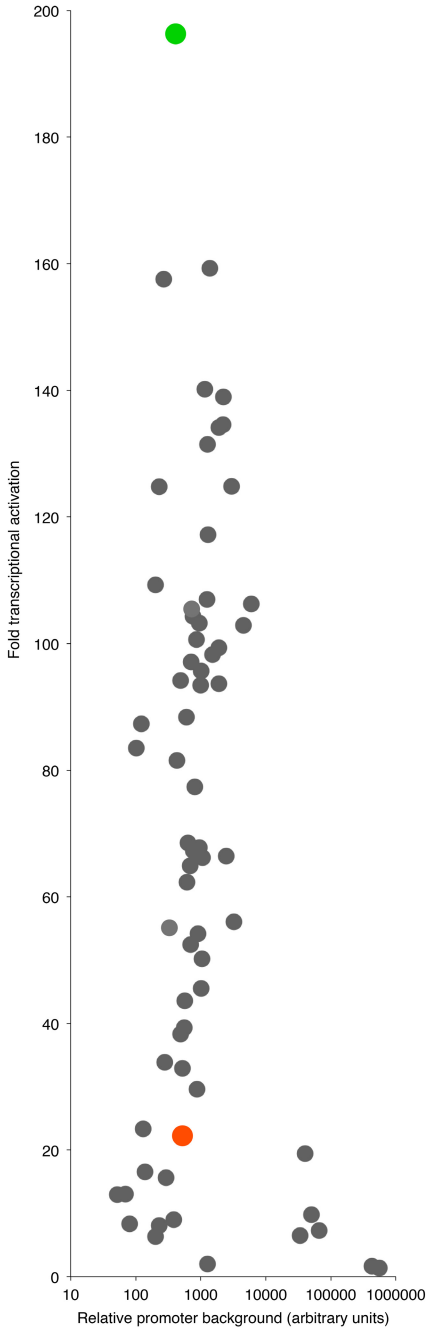

Extended Data Figure 2 | Optimization of the P_{lacZ} promoter for improved sensitivity and dynamic range. a, Promoter and DNA-binding domain combinations tested during P_{lacZ} optimization, showing uninduced and induced levels of absorbance-normalized luminescence. The SH2/HA4 interaction pair was used in all cases. The fold activation in each case was calculated as the ratio of the induced and uninduced luciferase expression signals. **b**, Graphical representation of the data in **a**, showing the wide distribution of promoter background levels and degrees of transcriptional activation. In **a** and **b**, the red and green dots indicate the starting (P_{lac62}) and final ($P_{lacZ\text{-}opt}$) promoter/DNA-binding domain combinations, respectively. Each data point in **b** reflects the average of at least three independent biological replicates.

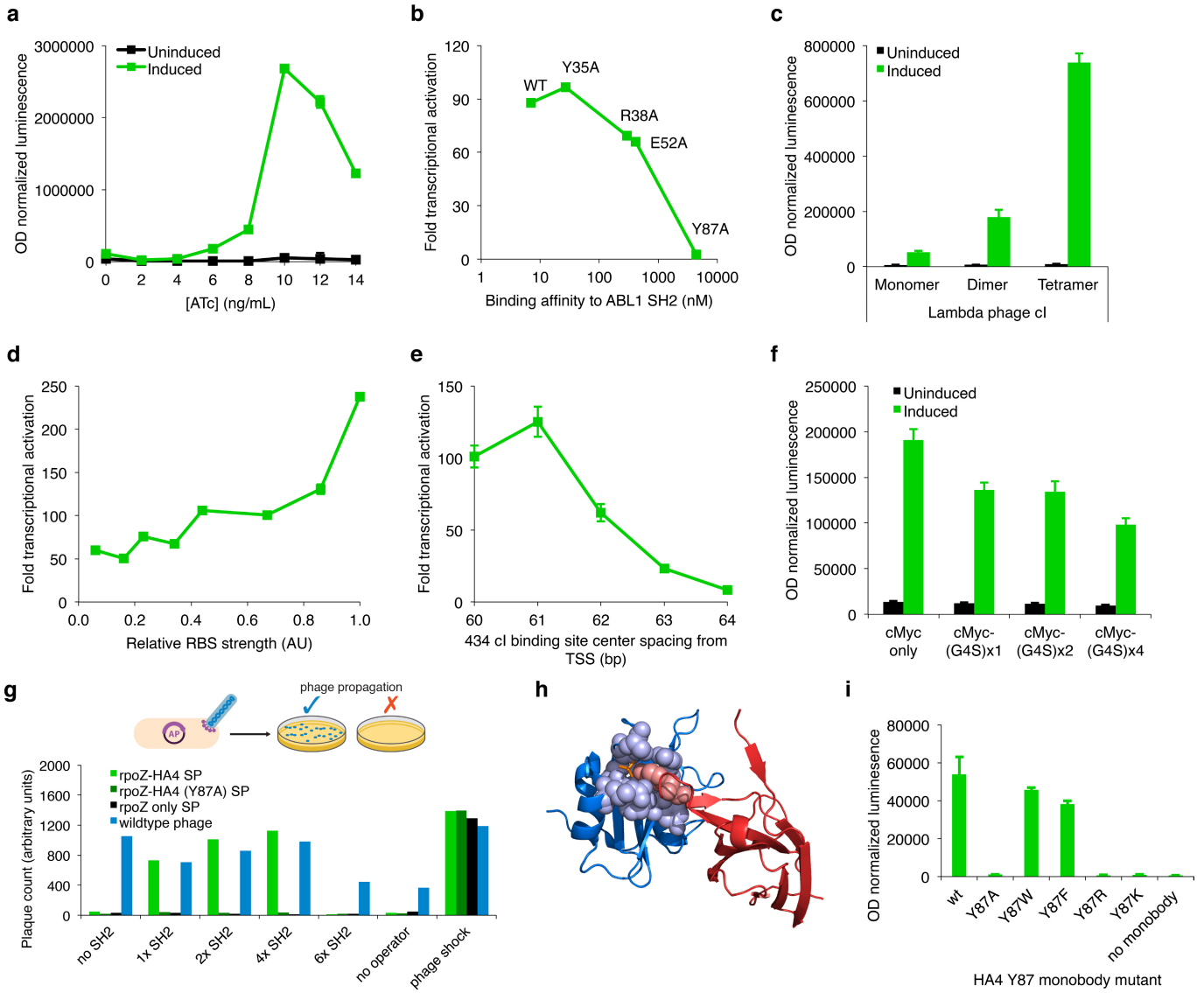

Extended Data Figure 3 | Bacterial two-hybrid optimization. a, Inducer titration of the interacting fusion proteins driving the two-hyrbid system. The black and green lines represent the uninduced (0 μM IPTG) and induced (1 μM IPTG) levels of IPTG-inducible *434cI–SH2* expression, while ATc induces expression of the *rpoZ–HA4* cassette. In subsequent graphs and assays, the expression level resulting from the IPTG-inducible P_{lac} promoter was measured by western blot and approximated using a constitutive promoter to reduce experimental variability. **b**, Degree of transcriptional activation using HA4 monobody mutants correlated with known binding affinities. The highest levels of activation resulted from K_d = low nanomolar affinities, while weak affinities in the K_d = low micromolar range could still be detected. **c**, Relationship between DNA-binding domain multivalency state (monomeric, dimeric, or tetrameric DNA-binding domain fused to the SH2 domain) and transcriptional activation resulting from the SH2/HA4 interaction, with higher multivalency states yielding greater activation levels. **d**, RBS modification enables robust modulation of the relative activation levels from the $P_{lacZ\text{-}opt}$ promoter using the SH2/HA4 interaction. **e**, Operator–promoter binding site spacing strongly affects transcriptional activation levels; 434cI binding at 61 base pairs upstream of the $P_{lacZ\text{-}opt}$ promoter resulted in the most robust activation. **f**, Linker extension to include one, two, or three G_4S motifs result in reduced activation levels using the SH2/HA4 interacting pair. **g**, Phage plaque formation as a function of target protein multivalency. 'No operator' indicates a scrambled 434cI operator control accessory plasmid; 'phage control' indicates an accessory plasmid in which the phage shock promoter (activated by phage infection) drives gene III expression. **h**, Co-crystal structure of the ABL1 SH2 (blue) bound to the HA4 monobody (red), highlighting the interaction of HA4 Y87 (red spheres) with key residues of the phosophotyrosine-binding pocket (blue spheres) of the SH2 domain (Protein Data Bank accession number 3K2M). The phosphate ion is shown in orange at the interaction interface. **i**, Apparent binding activity of mutants of the HA4 monobody at position 87. Tyrosine, tryptophan, and phenylalanine are tolerated at position 87 and enable protein–protein interaction by bacterial two-hybrid assay. Error bars, s.d. of at least three independent biological replicates.

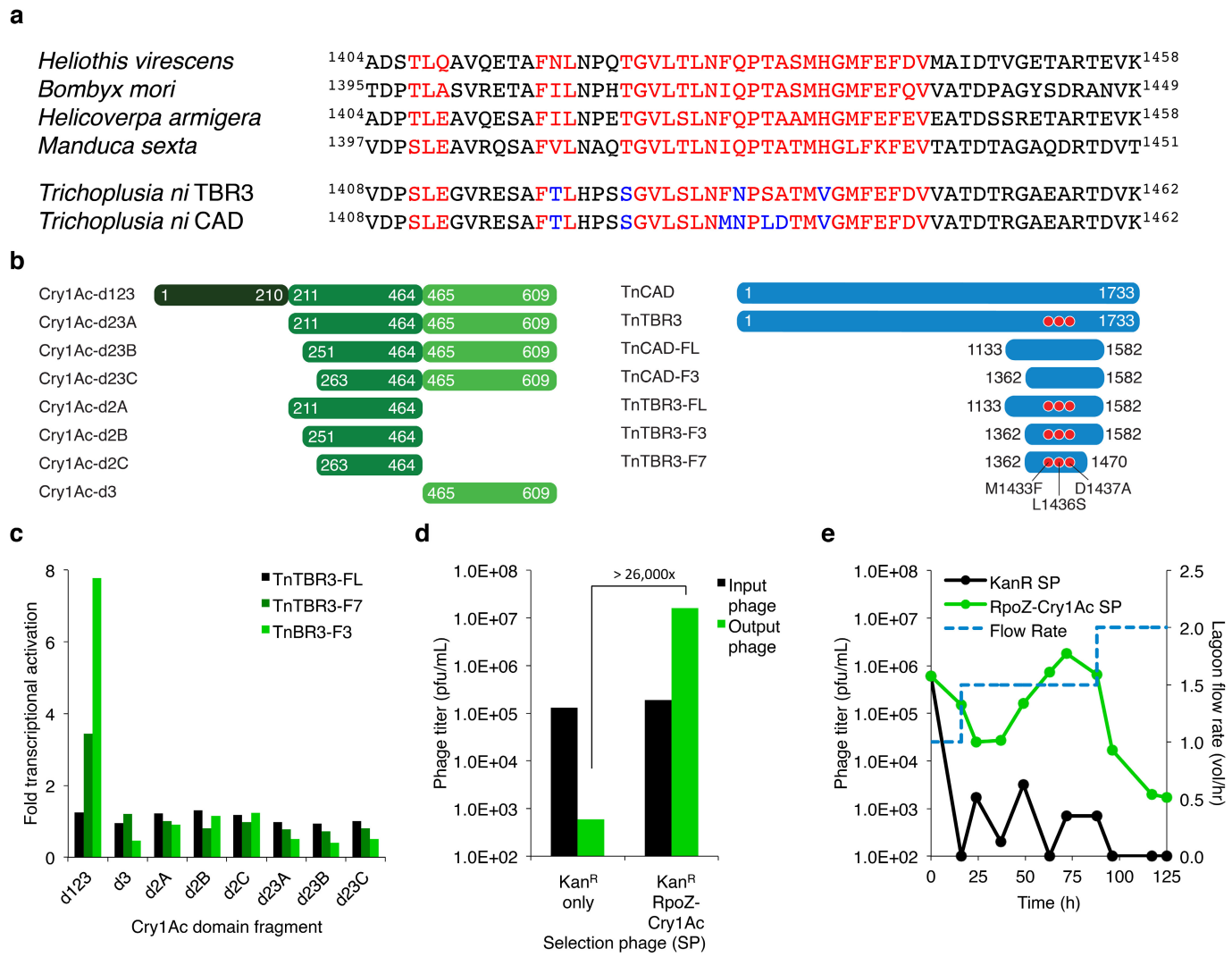

Extended Data Figure 4 | Choice of Cry1Ac and TnTBR3 fragments used in PACE. a, Protein sequence alignment of known Cry1Ac-binding motifs from cadherin receptors in several lepidopteran species, as well as the cadherin receptor from *T. ni* (TnCAD). The toxin-binding region (TBR; shown in red) of the known Cry1Ac-binding motifs differs from TnCAD at seven positions (shown in blue). Mutation of three residues in the TnCAD TBR (M1433F, L1436S, and D1437A) to resemble the corresponding positions of the cadherin-receptor TBRs yielded the evolutionary stepping-stone target TnTBR3. **b**, Schematic representations of the Cry1Ac and *T. ni* TBR3/CAD full-length receptors and fragments tested in this study. The red stars in the TnTBR3 variants represent the three mutations introduced into TnCAD to generate TnTBR3. **c**, Transcriptional activation assay using Cry1Ac and TnTBR3 fragments shows that the greatest degree of transcriptional activation resulted from full-length Cry1Ac together with TBR3 fragment 3 (TnTBR3-F3). RpoZ–Cry1Ac and 434cI–TnTBR3 fusions were used in all cases. **d**, Overnight phage enrichment assays using selection phages that encode either kanamycin resistance (Kan^R) only or Kan^R together with RpoZ–Cry1Ac. Compared with the Kan^R-only selection phage, the RpoZ–Cry1Ac selection phage enriches >26,000-fold overnight. **e**, Continuous propagation assays in the PACE format using either the Kan^R-only selection phage or the RpoZ–Cry1Ac selection phage show that the moderate affinity of Cry1Ac for TnTBR3 allows phage propagation at low flow rates (≤1.5 lagoon volumes per hour).

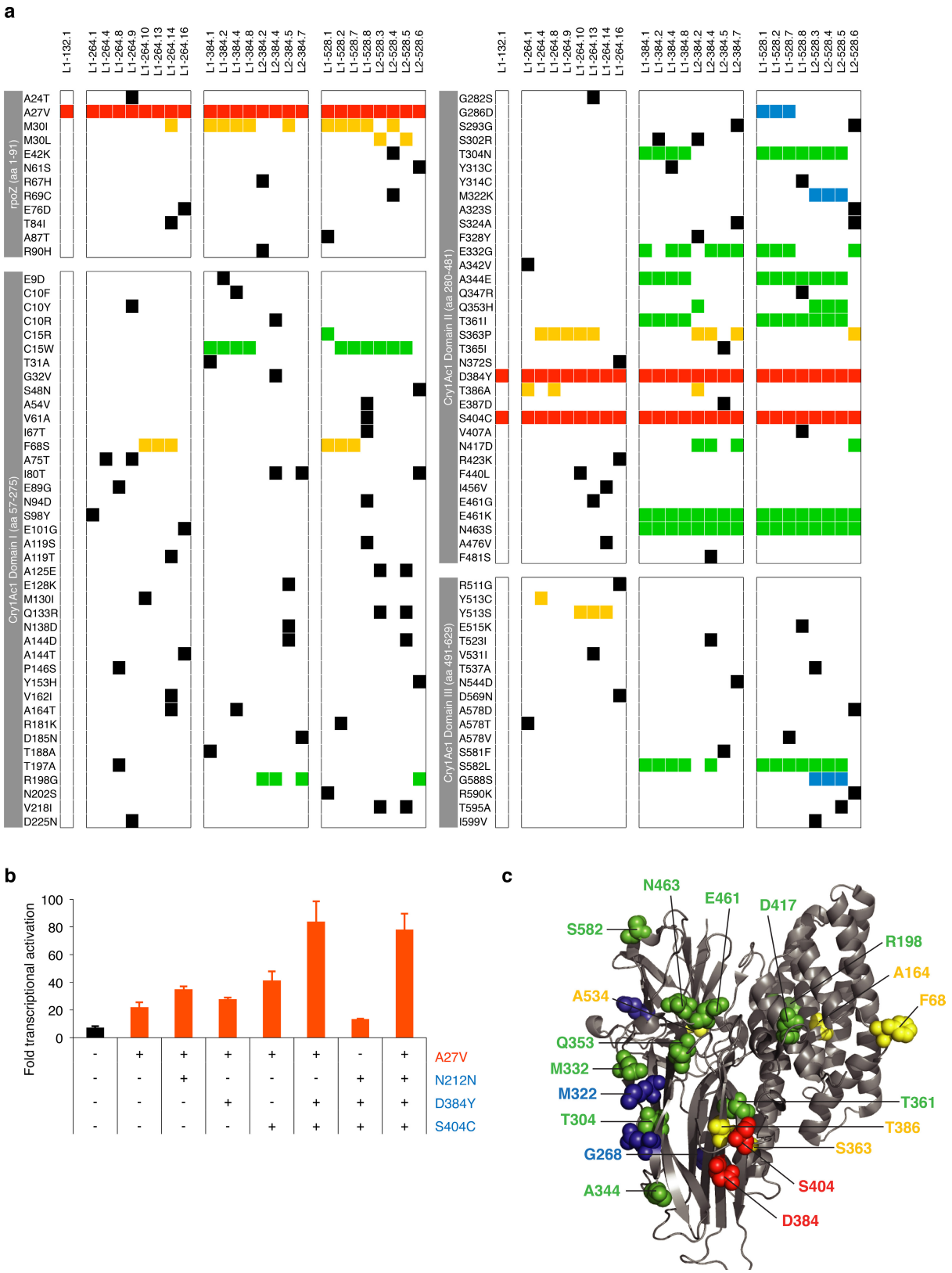

Extended Data Figure 5 | Single-clone sequencing and evolved Cry1Ac characterization after PACE using the bacterial two-hybrid luminescence reporter. a, Coding mutations of the tested RpoZ–Cry1Ac clones at the end of each of the four segments of PACE. Consensus mutations are coloured according to the segment in which they became highly enriched in the population (Fig. 3a). Mutations coloured in black were observed at low abundance (≤5% of sequenced clones). **b**, Mutational dissection of the consensus mutations from the first segment of PACE reveals the requirement for both D384Y and S404C to achieve high-level transcriptional activation using the TnTBR3-F3 target. Mutations listed in red occurred in the RpoZ activation domain, whereas mutations listed in blue occurred in the Cry1Ac domain. Error bars, s.d. of at least three independent biological replicates. **c**, Structure of wild-type Cry1Ac (Protein Data Bank accession number 4ARX) showing the positions of the evolved consensus mutations. The colours correspond to the PACE segments shown in Fig. 3 during which the mutations became highly abundant.

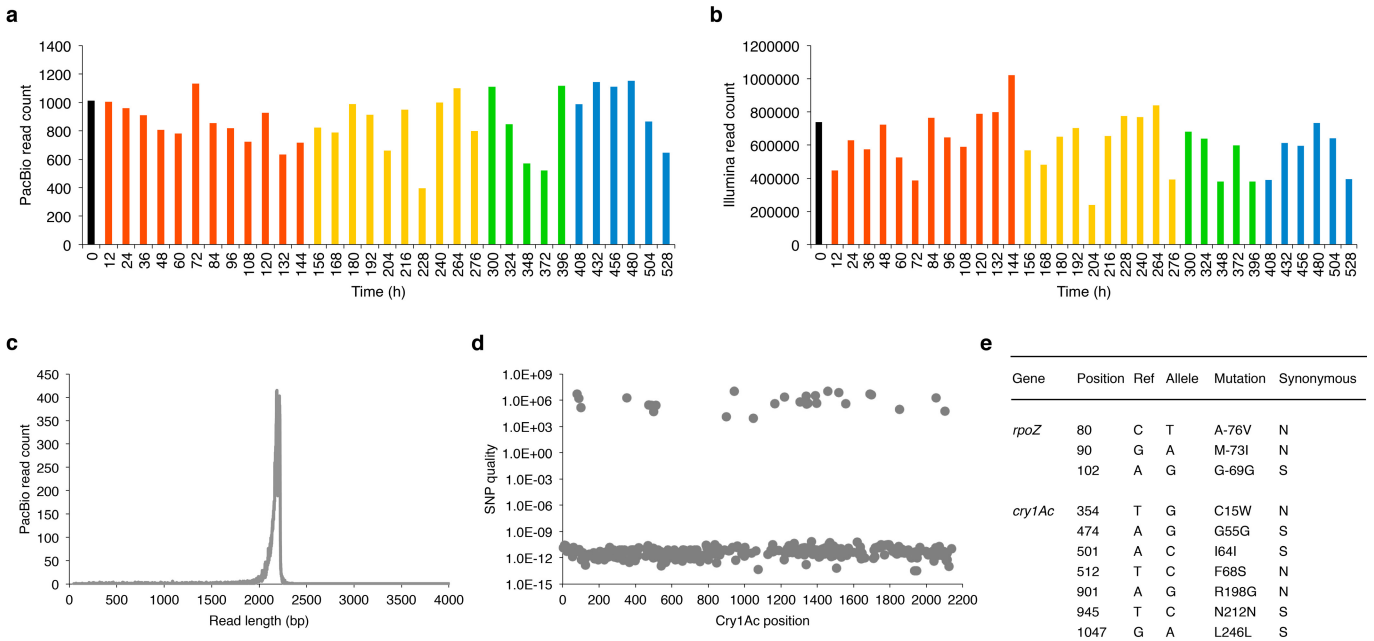

e

Gene	Position	Ref	Allele	Mutation	Synonymous
rpoZ	80	C	T	A-76V	N
	90	G	A	M-73I	N
	102	A	G	G-69G	S
cry1Ac	354	T	G	C15W	N
	474	A	G	G55G	S
	501	A	C	I64I	S
	512	T	C	F68S	N
	901	A	G	R198G	N
	945	T	C	N212N	S
	1047	G	A	L246L	S
	1166	G	A	G286D	N
	1220	C	A	T304N	N
	1304	A	G	E332G	N
	1340	C	A	A344E	N
	1344	T	C	A345A	S
	1349	A	G	Q347R	N
	1391	C	T	T361I	N
	1396	T	C	S363P	N
	1459	G	T	D384Y	N
	1519	A	T	S404C	N
	1558	A	G	N417D	N
	1690	G	A	E461K	N
	1697	A	G	N463S	N
	1852	G	A	E515K	N
	2054	C	T	S582L	N

Extended Data Figure 6 | High-throughput DNA sequencing of PACE Cry1Ac selection phage libraries. The number of reads mapped to the wild-type *rpoZ–Cry1Ac* reference sequence using (**a**) Pacific Biosciences (PacBio) or (**b**) Illumina sequencing. Time points are coloured according to the corresponding segment of the PACE experiment (Fig. 3a). **c**, In general, most PacBio reads aligned to the wt *rpoZ–Cry1Ac* reference sequence were found to cluster around ~2,200 base pairs, corresponding to the size of the full-length fusion gene and indicating high-quality sequencing reads. **d**, Illumina high-throughput sequencing yielded several high-quality single nucleotide polymorphisms across all time points. The corresponding mutations are shown in **e**.

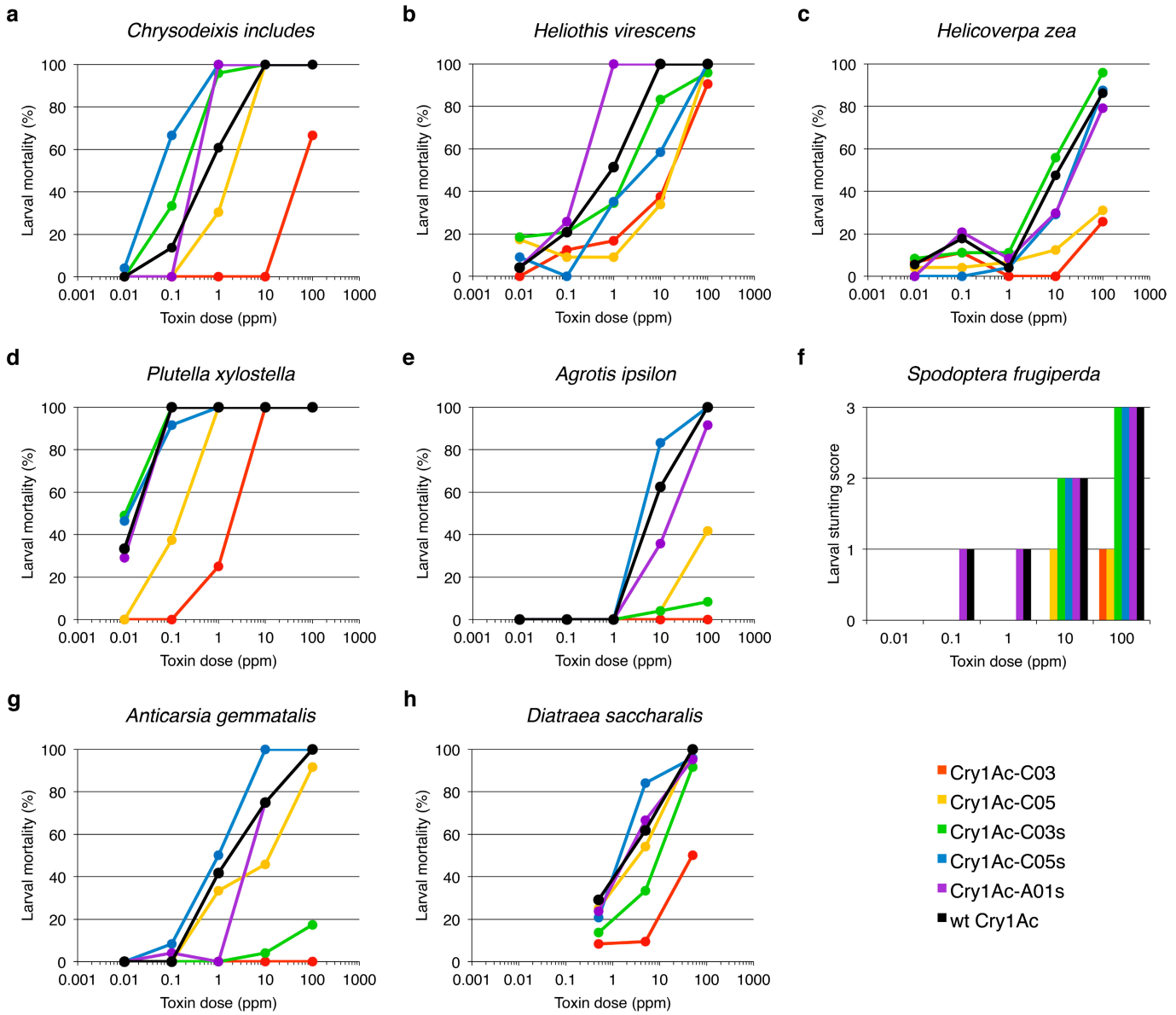

Extended Data Figure 7 | Insect diet bioassay activity of PACE-evolved Cry1Ac variants against various agricultural pests. Two consensus and three stabilized PACE-evolved Cry1Ac variants were tested for activity in eleven pests: **a**, *C. includes* (soybean looper); **b**, *Heliothis virescens* (tobacco budworm); **c**, *Helicoverpa zea* (corn earworm); **d**, *Plutella xylostella* (diamondback moth); **e**, *Agrotis ipsilon* (black cutworm); **f**, *Spodoptera frugiperda* (fall armyworm); **g**, *Anticarsia gemmatalis* (velvetbean caterpillar); **h**, *Diatraea saccharalis* (sugarcane borer); *Spodoptera eridania* (southern armyworm); *Leptinotarsa decemlineata* (Colorado potato beetle); and *Lygus lineolaris* (tarnished plant bug). Stabilized variants showed enhanced activity in *C. includens* and *H. virescens* compared with wild-type Cry1Ac, and comparable activity to wild-type Cry1Ac in *H. zea*, *P. xylostella*, *A. ipsilon*, *S. frugiperda*, *A. gemmatalis*, and *D. saccharalis*. No activity was observed for any of the Cry1Ac variants at any tested dose for *S. eridania*, *L. decemlineata*, or *L. lineolaris*. No insect larvae mortality was observed for *S. frugiperda*, although high toxin doses greatly stunted growth.

a

	T. ni	*C. includens*	*H. virescens*	*H. zea*	*P. xylostella*	*A. ipsilon*	*S. frugiperda*	*L. decemlineata*	*D. virgifera*
T. ni	-	78.6 (1362)	57.9 (1004)	57.3 (993)	53.1 (920)	51.8 (897)	51.2 (888)	25.6 (443)	26.1 (453)
C. includens	76.8 (1362)	-	55.7 (988)	54 (958)	51.8 (918)	49.9 (884)	49.8 (883)	24.6 (437)	25.5 (452)
H. virescens	58 (1004)	57 (988)	-	84.5 (1464)	55.4 (959)	58.9 (1021)	57.3 (992)	26 (451)	25.7 (445)
H. zea	57.4 (993)	55.4 (958)	84.6 (1464)	-	54.6 (945)	58.7 (1016)	57.3 (992)	26.3 (455)	25.4 (439)
P. xylostella	53.6 (920)	53.5 (918)	55.9 (959)	55 (945)	-	49.4 (848)	50.5 (867)	24.6 (422)	25.3 (435)
A. ipsilon	51 (897)	50.2 (884)	58 (1021)	57.7 (1016)	48.2 (848)	-	53.1 (935)	24 (422)	25 (440)
S. frugiperda	51.2 (888)	50.9 (883)	57.2 (992)	57.2 (992)	50 (867)	53.9 (935)	-	25.7 (445)	25.1 (436)
L. decemlineata	26.3 (443)	25.9 (437)	26.7 (451)	27 (455)	25 (422)	25 (422)	26.4 (445)	-	39.6 (668)
D. virgifera	26.8 (453)	26.8 (452)	26.4 (445)	26 (439)	25.8 (435)	26.1 (440)	25.8 (436)	39.6 (668)	-

b

	T. ni	*C. includens*	*H. virescens*	*H. zea*	*P. xylostella*	*A. ipsilon*	*S. frugiperda*	*L. decemlineata*	*D. virgifera*
T. ni	-	76.9 (170)	55.2 (122)	54.3 (120)	52 (115)	47.5 (105)	47.1 (104)	24 (53)	22.2 (49)
C. includens	75.2 (170)	-	51.3 (116)	51.3 (116)	47.8 (108)	42.5 (96)	42.5 (96)	22.6 (51)	22.6 (51)
H. virescens	55 (122)	52.3 (116)	-	81.5 (181)	50 (111)	49.5 (110)	47.7 (106)	23.4 (52)	19.8 (44)
H. zea	53.8 (120)	52 (116)	81.2 (181)	-	49.3 (110)	50.2 (112)	47.5 (106)	24.2 (54)	19.3 (43)
P. xylostella	52 (115)	48.9 (108)	50.2 (111)	49.8 (110)	-	43.9 (97)	48 (106)	22.2 (49)	19 (42)
A. ipsilon	47.3 (105)	43.2 (96)	49.5 (110)	50.5 (112)	43.7 (97)	-	42.8 (95)	18.5 (41)	18.9 (42)
S. frugiperda	46.8 (104)	43.2 (96)	47.7 (106)	47.7 (106)	47.7 (106)	42.8 (95)	-	24.8 (55)	23.4 (52)
L. decemlineata	22.3 (53)	21.4 (51)	21.8 (52)	22.7 (54)	20.6 (49)	17.2 (41)	23.1 (55)	-	38.2 (91)
D. virgifera	20.2 (49)	21 (51)	18.1 (44)	17.7 (43)	17.3 (42)	17.3 (42)	21.4 (52)	37.4 (91)	-

< 40%
< 70%
> 70%

Extended Data Figure 8 | Comparison of cadherin receptor sequence identity. The percentage sequence identity using the full-length cadherin receptor (**a**) or fragment used for directed evolution experiments (**b**) for insects tested in Extended Data Fig. 7. Numbers in parentheses denote the number of identical amino acids between the two receptors. In general, mortality and stunting data from diet bioassays correlate with cadherin receptor sequence identity.

Extended Data Table 1 | Insect bioassays against susceptible and resistant *T. ni*

		Toxin	LC_{50} (ppm)	95% CL	Slope	SE	Relative potency (%)
Susceptible *T. ni*	Mortality	Cry1Ac	0.039	0.019 - 0.069	2.54	0.26	100
		Cry1Ac-C03	0.793	0.505 - 1.082	2.84	0.41	5
		Cry1Ac-C05	0.715	0.407 - 1.176	1.78	0.22	5
		Cry1Ac-C03s	0.018	0.014 - 0.020	4.68	0.75	217
		Cry1Ac-C05s	0.035	0.026 - 0.045	3.59	0.41	111
		Cry1Ac-A01s	0.021	0.015 - 0.024	4.82	1.09	186
		Toxin	**IC_{50} (ppm)**	**95% CL**	**Slope**	**SE**	**Relative potency (%)**
	Growth inhibition	Cry1Ac	0.019	0.011 - 0.027	3.09	0.39	100
		Cry1Ac-C03	0.136	0.110 - 0.160	4.00	0.62	14
		Cry1Ac-C05	0.217	0.167 - 0.268	2.59	0.32	9
		Cry1Ac-C03s	0.007	0.003 - 0.010	3.65	0.61	271
		Cry1Ac-C05s	0.016	0.014 - 0.018	5.53	0.82	119
		Cry1Ac-A01s	0.005	0.004 - 0.006	4.92	0.9	380
		Toxin	**LC_{50} (ppm)**	**95% CL**	**Slope**	**SE**	**Relative potency (%)**
Resistant *T. ni*	Mortality	Cry1Ac	51.229	9.929 - 90.241	1.89	0.36	100
		Cry1Ac-C03	408.713	263.629 - 680.973	0.81	0.1	13
		Cry1Ac-C05	235.698	79.467 - 510.323	1.12	0.15	22
		Cry1Ac-C03s	1.841	1.390 - 2.312	2.25	0.28	2783
		Cry1Ac-C05s	1.938	1.550 - 2.352	2.55	0.29	2643
		Cry1Ac-A01s	0.153	0.046 - 0.289	2.01	0.22	33483
		Toxin	**IC_{50} (ppm)**	**95% CL**	**Slope**	**SE**	**Relative potency (%)**
	Growth inhibition	Cry1Ac	23.402	4.587 - 46.512	1.49	0.25	100
		Cry1Ac-C03	56.626	40.600 - 75.685	1.84	0.21	41
		Cry1Ac-C05	47.232	20.236 - 90.729	1.16	0.12	50
		Cry1Ac-C03s	0.733	0.515 - 0.949	2.06	0.28	3193
		Cry1Ac-C05s	1.116	0.797 - 1.484	2.19	0.23	2097
		Cry1Ac-A01s	0.083	0.061 - 0.104	2.57	0.38	28195

The LC_{50} and IC_{50} values were determined using seven to eight concentrations of the indicated toxins in an insect diet surface overlay bioassay using either Cry1Ac-susceptible or Cry1Ac-resistant *T. ni* neonatal larvae. Each toxin concentration was tested in five replicates, each of which contained ten randomly selected neonatal larvae. In each case, the 95% confidence interval (95% CI), the slope of the best fit (Slope) and the standard error (s.e.) is given. The relative potency (%) has been normalized to the activity of wild-type Cry1Ac for each case.

Extended Data Table 2 | Plasmids used in this work

Plasmid name	Class (resistance)	Origin of replication	ORF 1		ORF 2		ORF 3		Figure(s)
			Promoter	Gene	Promoter	Gene	Promoter	Gene	
pAB029f	CP (spec^R)	ColEI	P_{lacZ}	λcI-SH2$_{ABL1}$	P_{laclq}	lacI	-	-	S1A, S1C
pAB030g	AP (carb^R)	SC101	P_{lac62}	gIII, luxAB	P_{tet}	rpoA-HA4	-	-	S1A
pAB031a	CP (spec^R)	ColEI	P_{lacZ}	HA4-Zif268	P_{laclq}	lacI	-	-	S1B
pAB035a	AP (carb^R)	SC101	P_{lac62}	gIII, luxAB	P_{tet}	rpoZ-SH2$_{ABL1}$	-	-	S1B
pAB035h	AP (carb^R)	SC101	P_{lac62}	gIII, luxAB	P_{tet}	rpoZ-HA4	-	-	S1A, S1C
pAB042a	AP (carb^R)	SC101	P_{lac62}	gIII, luxAB	P_{tet}	rpoZ-YSX1	-	-	S1C
pAB042b	AP (carb^R)	SC101	P_{lac62}	gIII, luxAB	P_{tet}	rpoZ-MBPoff7	-	-	S1C
pAB042d	AP (carb^R)	SC101	P_{lac62}	gIII, luxAB	P_{tet}	rpoZ-p38_2_3	-	-	S1C
pAB043a	CP (spec^R)	ColEI	P_{lacZ}	λcI-MBP	P_{laclq}	lacI	-	-	S1C
pAB043c	CP (spec^R)	ColEI	P_{lacZ}	λcI-p38α	P_{laclq}	lacI	-	-	S1C
pAB045a	CP (spec^R)	ColEI	P_{lacZ}	rpoZ-HA4	P_{laclq}	lacI	-	-	S1B, S3A, S3C
pAB049b	CP (spec^R)	ColEI	P_{lacZ}	HA4-AsiA	P_{laclq}	lacI	-	-	S1A
pAB051e	AP (carb^R)	SC101	$P_{Ext\text{-}10consλop\text{-}62}$	gIII, luxAB	P_{tet}	λcI-SH2$_{ABL1}$	P_{lpp}	rpoD (R541C/F563Y/L607P)	S1A
pAB060c	AP (carb^R)	SC101	P_{lac62}	luxAB	P_{pro1}	λcI-SH2$_{ABL1}$	-	-	S1B
pAB061i	CP (spec^R)	ColEI	P_{pro1}	rpoZ-HA4	P_{laclq}	lacI	-	-	2A, S4B
pAB061i10	CP (spec^R)	ColEI	P_{pro1}	rpoZ-HA4 (Y87R)	P_{laclq}	lacI	-	-	S4B
pAB061i11	CP (spec^R)	ColEI	P_{pro1}	rpoZ-HA4 (Y87K)	P_{laclq}	lacI	-	-	S4B
pAB061i2	CP (spec^R)	ColEI	P_{pro1}	rpoZ-HA4 (Y87A)	P_{laclq}	lacI	-	-	2A, S4B
pAB061i3	CP (spec^R)	ColEI	P_{pro1}	rpoZ	P_{laclq}	lacI	-	-	2A, S4B
pAB061i8	CP (spec^R)	ColEI	P_{pro1}	rpoZ-HA4 (Y87W)	P_{laclq}	lacI	-	-	S4B
pAB061i9	CP (spec^R)	ColEI	P_{pro1}	rpoZ-HA4 (Y87F)	P_{laclq}	lacI	-	-	S4B
pAB064d	AP (carb^R)	SC101	P_{lac62}	luxAB	P_{pro1}	434cI-SH2$_{ABL1}$	-	-	S1B
pAB076i3	AP (carb^R)	SC101	$P_{lacZ\text{-}opt}$ (OR1)	gIII, luxAB	P_{pro1}	434cI-SH2$_{ABL1}$	-	-	2B
pAB076i5	AP (carb^R)	SC101	$P_{lacZ\text{-}opt}$ (OR1+2+3)	gIII, luxAB	P_{pro1}	434cI-SH2$_{ABL1}$	-	-	2B
pAB076i6	AP (carb^R)	SC101	$P_{lacZ\text{-}opt}$ (no operator)	gIII, luxAB	P_{pro1}	434cI-SH2$_{ABL1}$	-	-	2B
pAB076i7	AP (carb^R)	SC101	$P_{lacZ\text{-}opt}$ (OR1)	gIII, luxAB	P_{pro1}	434cI(RR69)-SH2$_{ABL1}$	-	-	2B
pAB078d10	AP (carb^R)	SC101	$P_{lacZ\text{-}opt}$ (OR1)	luxAB	P_{pro1}	434cI(RR69)-SH2$_{ABL1}$	-	-	2A, S3C
pAB078d3	AP (carb^R)	SC101	$P_{lacZ\text{-}opt}$ (OR1)	luxAB	P_{pro1}	434cI-SH2$_{ABL1}$	-	-	2A, S3B, S3C, S4B
pAB078d5	AP (carb^R)	SC101	$P_{lacZ\text{-}opt}$ (OR1)	luxAB	P_{pro1}	434cI	-	-	2A
pAB078d7	AP (carb^R)	SC101	$P_{lacZ\text{-}opt}$ (off-target)	luxAB	P_{pro1}	434cI-SH2$_{ABL1}$	-	-	2A
pAB078d8	AP (carb^R)	SC101	$P_{lacZ\text{-}opt}$ (OR1+2)	luxAB	P_{pro1}	434cI-SH2$_{ABL1}$	-	-	2A, S3C
pAB078d9	AP (carb^R)	SC101	$P_{lacZ\text{-}opt}$ (OR1+2+3)	luxAB	P_{pro1}	434cI-SH2$_{ABL1}$	-	-	2A
pAB082a	CP (spec^R)	ColEI	P_{pro1}	rpoZ-Cry1Ac-d123	-	-	-		S5C
pAB082b	CP (spec^R)	ColEI	P_{pro1}	rpoZ-Cry1Ac-d3	-	-	-		S5C
pAB082c	CP (spec^R)	ColEI	P_{pro1}	rpoZ-Cry1Ac-d2A	-	-	-		S5C
pAB082d	CP (spec^R)	ColEI	P_{pro1}	rpoZ-Cry1Ac-d2B	-	-	-		S5C
pAB082e	CP (spec^R)	ColEI	P_{pro1}	rpoZ-Cry1Ac-d2C	-	-	-		S5C
pAB082f	CP (spec^R)	ColEI	P_{pro1}	rpoZ-Cry1Ac-d23A	-	-	-		S5C
pAB082g	CP (spec^R)	ColEI	P_{pro1}	rpoZ-Cry1Ac-d23B	-	-	-		S5C
pAB082h	CP (spec^R)	ColEI	P_{pro1}	rpoZ-Cry1Ac-d23C	-	-	-		S5C
pAB085c	AP (carb^R)	SC101	$P_{lacZ\text{-}opt}$ (OR1)	luxAB	P_{tet}	434cI-TnTBR3-FL	-		S5C
pAB085d	AP (carb^R)	SC101	$P_{lacZ\text{-}opt}$ (OR1)	luxAB	P_{tet}	434cI-TnTBR3-F3	-		S5C
pAB085d6	AP (carb^R)	SC101	$P_{lacZ\text{-}opt}$ (OR1)	luxAB	P_{pro1}	434cI-TnTBR3-F3	-	-	3B
pAB085d7	AP (carb^R)	SC101	$P_{lacZ\text{-}opt}$ (OR1)	luxAB	P_{pro1}	434cI-TnCAD-F3	-	-	3C
pAB085e	AP (carb^R)	SC101	$P_{lacZ\text{-}opt}$ (OR1)	luxAB	P_{tet}	434cI-TnTBR3-F7	-		S5C
pAB088c	AP (carb^R)	SC101	$P_{lacZ\text{-}opt}$ (OR1)	gIII, luxAB	P_{pro1}	434cI-TnTBR3-F3	-	-	3A
pAB088e	AP (carb^R)	SC101	$P_{lacZ\text{-}opt}$ (OR1+2)	gIII, luxAB	P_{pro1}	434cI-TnTBR3-F3	-	-	3A
pAB088h	AP (carb^R)	SC101	$P_{lacZ\text{-}opt}$ (OR1+2)	gIII, luxAB	P_{pro1}	434cI-TnCAD-F3	-	-	3A
pAB088i	AP (carb^R)	SC101	$P_{lacZ\text{-}opt}$ (OR1)	gIII, luxAB	P_{pro1}	434cI(RR69)-TnCAD-F3	-	-	3A
pAB092a	AP (carb^R)	SC101	$P_{lacZ\text{-}opt}$ (OR1+2)	gIII, luxAB	P_{pro1}	434cI-SH2$_{ABL1}$	-	-	2B
pAB094a	CP (spec^R)	ColEI	P_{BAD}	rpoZ-HA4	P_C	araC	-	-	S3B
pAB094b	CP (spec^R)	ColEI	P_{BAD}	rpoZ-HA4 (Y35A)	P_C	araC	-	-	S3B
pAB094c	CP (spec^R)	ColEI	P_{BAD}	rpoZ-HA4 (R38A)	P_C	araC	-	-	S3B
pAB094d	CP (spec^R)	ColEI	P_{BAD}	rpoZ-HA4 (E52A)	P_C	araC	-	-	S3B
pAB094e	CP (spec^R)	ColEI	P_{BAD}	rpoZ-HA4 (Y87A)	P_C	araC	-	-	S3B
pAB107a	AP (carb^R)	SC101	$P_{lacZ\text{-}opt}$ (OR1)	gIII, luxAB	P_{pro1}	434cI	-	-	2B
pJC175e	AP (carb^R)	SC101	P_{PSP}	gIII, luxAB	-	-	-	-	2B
SP013	SP (kan^R)	M13 f1	P_{gIII}	rpoZ	-	-	-		S5D, S5E
SP055	SP (kan^R)	M13 f1	P_{gIII}	rpoZ-Cry1Ac	-	-	-		3A, S5D, S5E
SP096	SP (none)	M13 f1	P_{gIII}	rpoZ-HA4	-	-	-	-	2B
SP097	SP (none)	M13 f1	P_{gIII}	rpoZ-HA4 (Y87A)	-	-	-	-	2B
SP098	SP (none)	M13 f1	P_{gIII}	rpoZ	-	-	-	-	2B
MP4	MP (chlor^R)	CloDF13	P_{BAD}	dnaQ926, dam, seqA	P_C	araC	-	-	3A
MP6	MP (chlor^R)	CloDF13	P_{BAD}	dnaQ926, dam, seqA, emrR, ugi, cda1	P_C	araC	-	-	3A
pMON101647	EP (chlor^R)	ColEI	P_{T7}	(none)	-	-	-	-	-
pMON101695	EP (chlor^R)	P15A	P_{T7}	MBP-TVMV	-	-	-	-	-
pMON133051	EP (chlor^R)	ColEI	P_{T7}	Cry1Ac	-	-	-	-	-
pMON251427	EP (kan^R)	ColEI	P_{T7}	TnTBR3-FL	-	-	-	-	-
IS0008	EP (kan^R)	ColEI	P_{T7}	TnCAD-FL	-	-	-	-	-
pMON262346	EP (chlor^R)	ColEI	P_{T7}	Cry1Ac	-	-	-	-	-

Each plasmid is defined by the plasmid class, antibiotic resistance, origin of replication, and promoter/gene combinations describing the relevant open reading frames carried by the plasmid. Relevant figures where these materials were used are given in each case.